

RESEARCH

Open Access



Ca²⁺-dependent H₂O₂ response in roots and leaves of barley - a transcriptomic investigation

Sabarna Bhattacharyya¹, Carissa Bleker², Bastian Meier³, Maya Giridhar⁴, Elena Ulland Rodriguez¹, Adrian Maximilian Braun¹, Edgar Peiter³, Ute C. Vothknecht^{1*} and Fatima Chigri^{1*}

Abstract

Background Ca²⁺ and H₂O₂ are second messengers that regulate a wide range of cellular events in response to different environmental and developmental cues. In plants, stress-induced H₂O₂ has been shown to initiate characteristic Ca²⁺ signatures; however, a clear picture of the molecular connection between H₂O₂-induced Ca²⁺ signals and H₂O₂-induced cellular responses is missing, particularly in cereal crops such as barley. Here, we employed RNA-seq analyses to identify transcriptome changes in roots and leaves of barley after H₂O₂ treatment under conditions that inhibited the formation of cytosolic Ca²⁺ transients. To that end, plasma membrane Ca²⁺ channels were blocked by LaCl₃ application prior to stimulation of barley tissues with H₂O₂.

Results We examined the expression patterns of 4246 genes that had previously been shown to be differentially expressed upon H₂O₂ application. Here, we further compared their expression between H₂O₂ and LaCl₃ + H₂O₂ treatment. Genes showing expression patterns different to the previous study were considered to be Ca²⁺-dependent H₂O₂-responsive genes. These genes, numbering 331 in leaves and 1320 in roots, could be classified in five and four clusters, respectively. Expression patterns of several genes from each cluster were confirmed by RT-qPCR. We furthermore performed a network analysis to identify potential regulatory paths from known Ca²⁺-related genes to the newly identified Ca²⁺-dependent H₂O₂ responsive genes, using the recently described Stress Knowledge Map. This analysis indicated several transcription factors as key points of the responses mediated by the cross-talk between H₂O₂ and Ca²⁺.

Conclusion Our study indicates that about 70% of the H₂O₂-responsive genes in barley roots require a transient increase in cytosolic Ca²⁺ concentrations for alteration in their transcript abundance, whereas in leaves, the Ca²⁺ dependency was much lower at about 33%. Targeted gene analysis and pathway modeling identified not only known components of the Ca²⁺ signaling cascade in plants but also genes that are not yet connected to stimuli-associated signaling. Potential key transcription factors identified in this study can be further analyzed in barley and other crops to ultimately disentangle the underlying mechanisms of H₂O₂-associated signal transduction mechanisms. This could

*Correspondence:
Ute C. Vothknecht
vothknecht@uni-bonn.de
Fatima Chigri
fchigri@uni-bonn.de

Full list of author information is available at the end of the article



© The Author(s) 2025. **Open Access** This article is licensed under a Creative Commons Attribution 4.0 International License, which permits use, sharing, adaptation, distribution and reproduction in any medium or format, as long as you give appropriate credit to the original author(s) and the source, provide a link to the Creative Commons licence, and indicate if changes were made. The images or other third party material in this article are included in the article's Creative Commons licence, unless indicated otherwise in a credit line to the material. If material is not included in the article's Creative Commons licence and your intended use is not permitted by statutory regulation or exceeds the permitted use, you will need to obtain permission directly from the copyright holder. To view a copy of this licence, visit <http://creativecommons.org/licenses/by/4.0/>.

aid breeding for improved stress resistance to optimize performance and productivity under increasing climate challenges.

Keywords ROS, Stress, RNA-Seq, Ca²⁺ signaling, Crosstalk, *Hordeum vulgare*

Introduction

To withstand short-term detrimental conditions, plants have evolved complex and efficient molecular machineries to monitor and respond to environmental cues. An early plant response to many forms of stress involves reactive oxygen species (ROS) as a purposefully generated signal to modulate crucial aspects of plant growth, development, and stress adaptation [1]. ROS also constitute inevitable by-products of aerobic metabolism that under normal physiological conditions are mainly produced at a low level; however, disruption of metabolic pathways during stress often results in a dramatic increase in their rate of production [2, 3]. Hydrogen peroxide (H₂O₂), a very stable ROS, is generated within different cellular compartments such as chloroplasts, mitochondria, and peroxisomes, as well as extra-cellularly in the apoplast [4]. H₂O₂ is generated either passively by metabolic pathways such as photosynthesis, photorespiration and respiration, or produced actively by oxidases like the respiratory burst oxidase homologs (RBOHs) [3]. Also, H₂O₂ can be transported between different cellular compartments, cells or even tissues for the purpose of removal or accumulation, and is now considered as an important player in long-distance-signaling [5, 6].

At low levels, H₂O₂ can be beneficial for the plant and act as a signal transduction molecule to achieve stress tolerance; however, it can cause cellular damage and programmed cell death at higher concentrations [7]. Hence, a strict balance between production and scavenging of H₂O₂ is essential to prevent its accumulation to toxic levels and to ensure its function as a signaling molecule. Plants have thus evolved a complex array of enzymatic and non-enzymatic detoxification systems to adjust the H₂O₂ homeostasis in all subcellular compartments [8, 9]. As signaling molecule, H₂O₂ is involved in the regulation of various developmental and physiological processes such as root system development [10, 11], flowering [12], seed germination [13], senescence [14] and stomatal aperture [15]. Additionally, studies have uncovered key roles for H₂O₂ as a second messenger in the signaling pathways associated with environmental stress responses in *Arabidopsis thaliana* and crop species such as drought [16, 17], salinity [18], heat [19, 20], UV radiation [21], ozone [22], chilling [23], heavy metal [24], and pathogens [25, 26]. Various stimuli can induce increases of H₂O₂ levels, known as the “oxidative burst”, which is subsequently sensed and transmitted to activate downstream processes including transcriptional reprogramming to elicit

appropriate adaptive stress responses [27]. Moreover, H₂O₂ can activate other signaling cascades involving secondary messengers such as nitric oxide, phytohormones, and Ca²⁺.

Ca²⁺ also plays a pivotal role in the regulation of various developmental processes and response to environmental stresses. Changes in cytosolic free Ca²⁺ concentrations ([Ca²⁺]_{cyt}) are one of the earliest cellular responses observed in plants to almost every biotic and abiotic stress that has been investigated, including salt [28, 29], cold [30, 31], drought [32–34], heat [35, 36], heavy metals [37], and pathogens [38, 39]. The transient changes in [Ca²⁺]_{cyt} are sensed and decoded by a toolkit of Ca²⁺ sensor proteins like calmodulins (CaMs), calmodulin-like proteins (CMLs), calcineurin B-like proteins (CBLs), and CBL-interacting protein kinases (CIPKs) as well as Ca²⁺-dependent protein kinases (CPKs/CDPKs) [40]. Like H₂O₂, Ca²⁺ signaling affects different cellular processes including regulation of gene transcription and associated downstream responses [41].

A crosstalk between Ca²⁺ and H₂O₂ signaling pathways has been shown in response to various abiotic and biotic stresses [42, 43]. A number of studies indicated that Ca²⁺ acts as an upstream component in H₂O₂ signaling by regulating H₂O₂ production. In plants, RBOHs possess a cytosolic N-terminal regulatory domain containing Ca²⁺-binding EF-hand motifs and Ca²⁺-dependent phosphorylation sites as targets for CPKs that are necessary for RBOH activation [44–46]. By contrast, there is also evidence that H₂O₂ acts as an upstream signal by inducing [Ca²⁺]_{cyt} transients involved in plant responses such as stomatal closure, programmed cell death, and other stress adaptation [47–49]. H₂O₂-induced Ca²⁺ release is likely due to the direct regulation of Ca²⁺-permeable channels. Annexins, cyclic nucleotide gated channels (CNGCs), and mechanosensitive ion channels (MSLs) have been proposed to function as H₂O₂-activated Ca²⁺ channels that mediate cellular Ca²⁺ influxes [50, 51]. In a recent study a H₂O₂-sensor in plants, H₂O₂-INDUCED CA²⁺ INCREASES 1 (HPCA1) was identified that mediates H₂O₂-induced activation of Ca²⁺ channels in guard cells leading to elevation in [Ca²⁺]_{cyt} and in turn initiation of stomatal closure [52]. Intriguingly, it has been shown that HPCA1 is required for systemic ROS- and Ca²⁺-mediated cell-to-cell signaling and that this includes the Ca²⁺ permeable channel MSL3 as well as the Ca²⁺ sensor CBL4 and its interacting protein kinase CIPK26 [51]. However, despite the large volume of reports and studies, it remains unclear how H₂O₂ and Ca²⁺ signals regulate

each other, what determines the directionality of the crosstalk, and what connects both signaling pathways to achieve their synergistic response.

We thus intended to identify the contribution of cytosolic Ca^{2+} signals to H_2O_2 -induced transcriptomic changes in leaves and roots of barley. Barley is an important global feed and food source and has been widely studied as a model for monocot crops due to its diploid nature and ease of cross-breeding [53, 54]. The effect of H_2O_2 on the transcriptome was recently elucidated in barley leaves and roots [55], revealing common as well as tissue-specific changes in transcript abundance of over 4000 genes including various transcription factors (TFs), genes associated with hormone pathways, and other vital functions such as photosynthesis, cell wall biogenesis, and H_2O_2 detoxification. It has also been shown that barley, as other plants, reacts to H_2O_2 application with a transient elevation in $[\text{Ca}^{2+}]_{\text{cyt}}$ [56]. For the comparative approach carried out in the current study, Ca^{2+} transients were pharmacologically inhibited by the well-known plasma membrane Ca^{2+} channel blocker LaCl_3 . RNA-seq analyses revealed that 1652 of the previously identified H_2O_2 responsive genes were fully or partially dependent on Ca^{2+} signals for their regulation since their differential expression was altered when the Ca^{2+} signal was inhibited by LaCl_3 . Subsequent network analyses provided testable hypotheses on the molecular mechanisms of the crosstalk between oxidative stress and Ca^{2+} signaling. Ultimately, understanding the underlying molecular processes of this crosstalk might increase our ability to improve stress resistance in barley and other crops to optimize performance and productivity under increasing climate challenges.

Materials and methods

Plant material, growth conditions, and stress treatment

Barley plants (*Hordeum vulgare* cultivar Golden Promise) were grown for five days in pots filled with water-soaked vermiculite in a climate-controlled growth chamber under long-day conditions with 16 h light at 20 °C and a light intensity of 120 $\mu\text{mol photons m}^{-2} \text{s}^{-1}$ (Philips TLD 18 W of alternating 830/840 light color temperature) and 8 h darkness at 18 °C. For stress treatments, five-day-old barley seedlings were removed from the pots and incubated in ddH₂O with or without 10 mM LaCl_3 for one hour, briefly rinsed and then treated with ddH₂O with or without 10 mM H_2O_2 for three hours. Seedlings were thoroughly rinsed before subsequent analyses.

H_2O_2 staining and microscopic analyses

A modified protocol from [57] was used to stain H_2O_2 in barley leaves and roots with 2',7'-dichlorodihydrofluorescein diacetate (H_2 -DCFDA; Thermo Fisher Scientific, USA). After stress treatment as described above,

the seedlings were washed carefully and treated with 10 μM H_2 -DCFDA in 0.25% DMSO in the dark for one hour, followed by vacuum infiltration for 1 min in a desiccator. Approximately 5 mm segments of both tissues were mounted on a slide using tape. The fluorescence of 2',7'-Dichlorofluorescein (DCF) was analyzed using a Leica SP8 Lightning confocal laser scanning microscope (Leica Microsystems, Germany) with an excitation wavelength of 488 nm and emission between 517 and 527 nm which was detected using a HyD Detector. Fluorescence signals were quantified in regions of interest (ROIs) using the integrated LASX software (Leica Microsystems, Germany).

Ca^{2+} measurements using genetically encoded

APOAEQUORIN

Effects of LaCl_3 on Ca^{2+} signals were analysed as previously described [56]. Hv-AEQ_{cyt} plants expressing *APOAEQUORIN* were grown for five days on water-soaked vermiculite as described above, and 5 mm sections from the tip of leaves and primary roots were reconstituted in 2.5 μM coelenterazine (Carl Roth, Germany) in ddH₂O in 96-well plates for 16 h in the dark. After reconstitution, the coelenterazine solution was replaced by ddH₂O with or without 1 mM LaCl_3 , and samples were placed for one hour in light before measurements. Baseline luminescence was recorded for 90 s with an integration time of 1 s in a plate luminometer (Mithras LB940, Berthold Technologies, Germany) before injection of an equal volume of a 2-fold-concentrated solution of H_2O_2 (final concentration 10 mM). Changes in luminescence were recorded for another 600 s before the injection of a 2-fold-concentrated discharge solution (final concentration 1 M CaCl_2 in 10% ethanol) and a subsequent recording of luminescence for 300 s. $[\text{Ca}^{2+}]_{\text{cyt}}$ was calculated as described in [48]. To calculate $\Delta[\text{Ca}^{2+}]_{\text{cyt}}$, the mean of $[\text{Ca}^{2+}]_{\text{cyt}}$ derived from 10 s of baseline prior to treatment was subtracted from the maximum increase of $[\text{Ca}^{2+}]_{\text{cyt}}$ obtained after injection.

RNA-sequencing and data analyses

After stress treatments as described above, plants were carefully washed with ddH₂O several times before roots and leaves were separated and ground into a fine powder under liquid nitrogen using mortar and pestle. Total RNA was isolated from the tissues using the Quick-RNA miniprep Kit (ZymoResearch, USA) following the manufacturer's instructions. The quality of RNA was assessed using a NABI Nanodrop UV/Vis Spectrophotometer (MicroDigital, South Korea). Integrity of the extracted RNA was confirmed by separation of the 28 S and 18 S rRNA bands on a 1% agarose gel.

RNA-seq was performed on three biological replicates for each treatment. Each replicate consisted of pooled

material from three plants. 3' mRNA sequencing including synthesis, labelling, and hybridization of cDNA was performed at the NGS core facility (Medical Faculty at the University of Bonn, Germany) using a NovaSeq6000 (Illumina, USA). cDNA library preparation was done using the QuantSeq protocol [58], where oligo dT priming was followed by complementary strand synthesis without any prior removal of ribosomal RNA. All further steps of data processing and alignment were performed as previously described [55]. Gene counts were approximated from the aligned files using the FeatureCounts function from the Rsubread package [59]. Differential expression analyses using the normalized counts were carried out using the DeSeq2 package [60], with default parameters for variance stabilizing transformations. The False Discovery Rate (FDR) cutoff for inclusion of data was set to 0.01. Principal Component Analyses (PCA) plots were generated with the gene counts for each sample using the princomp() function, in order to analyze and map the different variances obtained in this study. The volcano plots were made using ggplot2 and ggrepel packages of RStudio. A homology search against the genome of the model organism *A. thaliana* (TAIR 10) was performed using the Barley Reference Transcript (BaRTv1.0) dataset [61] available at www.ics.hutton.ac.uk with an E-value cutoff of $1e^{-30}$. K-means clustering analyses [62, 63] was carried out using the base k-means function on RStudio with the help of pre-defined clusters determined with the help of the gap statistic method [64]. The clustering analyses were performed separately for leaf and root tissues. The clusters were then represented as heatmaps using the pheatmap function.

Network analyses

Stress Knowledge Map is a plant molecular interaction resource, containing the Comprehensive Knowledge Network (CKN), a large, condition agnostic knowledge graph of molecular interactions in *A. thaliana* [65]. CKN was used to identify potential upstream regulators of the Ca^{2+} -dependent H_2O_2 responsive genes. The network was first filtered to only reliable interactions (rank 0 - highest reliability, rank 1, and rank 2 edges), and GoMapMan (GMM) [66] annotations used to extract genes known to be involved in Ca^{2+} signaling (171 nodes annotated with GMM terms “30.3 - signaling.calcium”, “34.21 - transport.calcium”, or “34.22 - transport.cyclic nucleotide or calcium regulated channels”) or know to be involved in redox signalling (119 nodes annotated with GMM terms “21.1 - redox.thioredoxin”, “21.2 - redox.ascorbate and glutathione”, “21.4 - redox.glutaredoxins”, or “21.5 - redox.peroxiredoxin”). Shortest paths from the known Ca^{2+} involvement (“source”) set to *A. thaliana* homologs of the newly identified Ca^{2+} -dependent H_2O_2 responsive genes (“target” set), with a maximum path length of

three were extracted from CKN. To improve the biological plausibility of the extracted paths, we required that only a single transcriptional regulatory interaction was present in each path, and it directly regulates the target. The shortest paths were filtered to the closest source(s) per target, and merged. The same approach was taken to identify paths from the known redox related (source) set to the *A. thaliana* homologs of the Ca^{2+} -independent H_2O_2 responsive genes. The analysis was performed in Python using Stress Knowledge Map (SKM) tools [65], the networkX library [67], and graph-tools [68]. Results were visualised in Cytoscape [69] using the py4cytoscape library [68, 70]. Code for the network analyses is available on GitHub (see Availability of data and materials). The Cytoscape session file is available as an additional file (Additional File 1).

cDNA synthesis and RT-qPCR

Synthesis of cDNA was carried out with 0.5–1 µg of total RNA using the ThermoFisher first strand cDNA synthesis kit with oligo-dT₁₈ primers (Thermo Fisher Scientific, USA) following the manufacturer’s instructions. The cDNA synthesis reaction was terminated by heating at 70 °C for five minutes. 1:5 dilutions of the cDNAs were used for amplification, with 2 µl of the diluted cDNA added to a total reaction volume of 10 µl. RT-qPCR was carried out on a BioRad CFX 96 real-time PCR detection system (Biorad, USA) with a reaction mixture consisting of SYBR Green PCR Mix (ThermoFisher Scientific, USA), forward and reverse primers (Table S1), ddH₂O, and the template cDNA. Transcript levels were calculated using the $2^{-\Delta\Delta Ct}$ method [71] after normalization against *HvACTIN* and *HvGAPDH*. Data analyses, including preparation of bar graphs followed by ANOVA and Tukey’s Post-Hoc multi comparison tests, were performed using the tidyverse and agricolae packages, respectively, in RStudio. Linear regression analyses were also performed for the RT-qPCR. The base lm () function was used for the analyses. Correlation analysis was additionally carried out with the Karl Pearson method, using the cor.test () function.

Results

Analysis of the transcriptional effects of H_2O_2 and $LaCl_3$ treatment in barley leaves and roots

In barley, it has been shown that the application of exogenous H_2O_2 induces increases in $[Ca^{2+}]_{cyt}$ in both leaves and roots [56]. To investigate the contribution of Ca^{2+} signaling in the H_2O_2 -induced transcriptomic changes, we performed RNA-seq analyses under conditions that inhibited H_2O_2 -induced Ca^{2+} transients. For that end, barley seedlings used for RNA-seq were pre-treated with the plasma membrane Ca^{2+} channel blocker $LaCl_3$ before application of H_2O_2 . Additionally, RNA-seq was

also performed on plants treated solely either with LaCl_3 or with ddH_2O . $\text{H}_2\text{-DCFDA}$ staining revealed increased H_2O_2 levels inside both leaves and roots of barley compared to control plants and that the pre-treatment with LaCl_3 had no effect on the H_2O_2 increase in both tissues (Fig. 1A-C). Furthermore, the inhibitory effect of LaCl_3 on H_2O_2 -induced changes in $[\text{Ca}^{2+}]_{\text{cyt}}$ was confirmed using transgenic barley reporter lines expressing the *APOAEQUORIN* reporter gene (Fig. 1D) in line with already published data [56].

RNA-seq analysis was carried out on three biological replicates per tissue and treatment, each comprising the pooled extracted RNA from three different plants. Approximately 13–15 million raw reads were

obtained and aligned against the barley reference genome (BaRTv1.0). The total alignment rate averaged from 70 to 80% across all the samples used in this study (Table 1). The aligned reads were used for differential expression analyses between the treatments and the ddH_2O -treated control. The homogeneity of the gene counts along with their associated variance across tissues and treatments was represented as a principal component analysis (PCA) plot (Fig. 2A). The highest percentage of variance was associated with the different tissues (PC1, X-axis), with slightly lesser variance associated with the treatments (PC2, Y-axis).

Differentially expressed genes (DEGs) between treatments and control (ddH_2O) were defined through

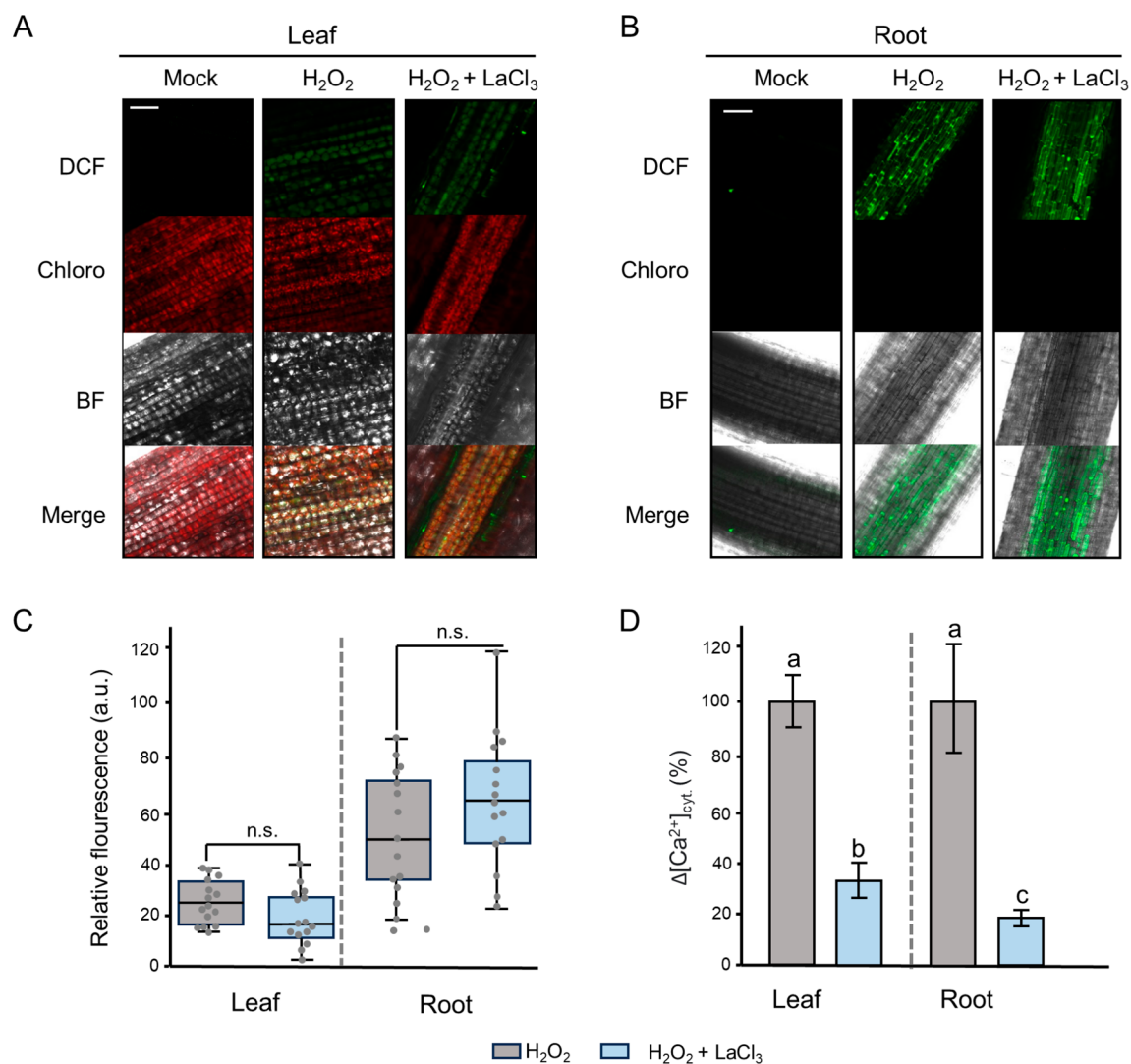


Fig. 1 Effects of LaCl_3 on the penetration of H_2O_2 and on H_2O_2 -induced Ca^{2+} signals in barley. Plants were pre-treated either with or without 1mM LaCl_3 before application of 10mM H_2O_2 . For visualization of H_2O_2 in **(A)** leaves and **(B)** roots of barley, H_2DCFDA staining was employed. BF: bright field, Chloro: Chlorophyll autofluorescence, DCF: Dichlorofluorescein, scale bar: 50 μm . **(C)** Quantification of relative DCF fluorescence using the LASX software. Values represent means \pm SE of three independent replicates with 5 ROIs each ($n = 15$). n.s.: non-significant changes, a.u.: arbitrary units. **(D)** Inhibition of H_2O_2 -induced Ca^{2+} signals in barley leaf and root tips under the effect of LaCl_3 . Values represent means \pm SE of three biological replicates ($n = 3$). Significances were estimated with one-way ANOVA and Tukey's Post-Hoc HSD analyses at $P < 0.05$ cutoff

Table 1 Summary of reads and alignment statistics. RNA-sequencing was carried out with three independent replicates. After quality control, reads were aligned against the barley reference genome (BaRTv1.0), and alignment files in bam format were then used for further processing

Sample	Replicate	Total Reads	Aligned Reads	Aligned Reads (%)
leaf LaCl ₃ + H ₂ O ₂	1	13,297,596	10,033,011	75.44
	2	13,122,889	10,246,998	78.08
	3	13,201,445	10,022,100	75.91
leaf LaCl ₃	1	12,787,648	9,420,291	73.70
	2	12,541,411	9,415,802	75.10
	3	14,111,932	10,538,682	74.70
root LaCl ₃ + H ₂ O ₂	1	14,455,626	10,715,747	74.12
	2	13,699,232	10,435,889	76.17
	3	13,599,945	10,166,184	74.75
root LaCl ₃	1	13,690,522	10,610,155	77.50
	2	12,208,414	9,302,812	76.20
	3	11,154,444	8,745,084	78.30

filtering with a cut-off of FDR < 0.01, while the other genes were considered as genes with unchanged transcript levels (UCs) (Table S2). Volcano plot analyses showed that combined H₂O₂ + LaCl₃ treatment resulted in a quite similar number of up- and down-regulated genes in leaves and roots with a total number of 1006 and 1344 DEGs detected, respectively (Fig. 2B; Table S2). From these DEGs we next omitted all the genes that showed similar differential expression upon treatment with LaCl₃ alone (Fig. S1; Table S2). Overall, this analysis identified 989 and 1001 DEGs in leaves and roots of barley, respectively, which are unique for the H₂O₂ + LaCl₃ treatment (Fig. 2C, Table S2). While the overall number of DEGs was similar for both tissues, the leaves had slightly more down- and the roots considerably more up-regulated DEGs.

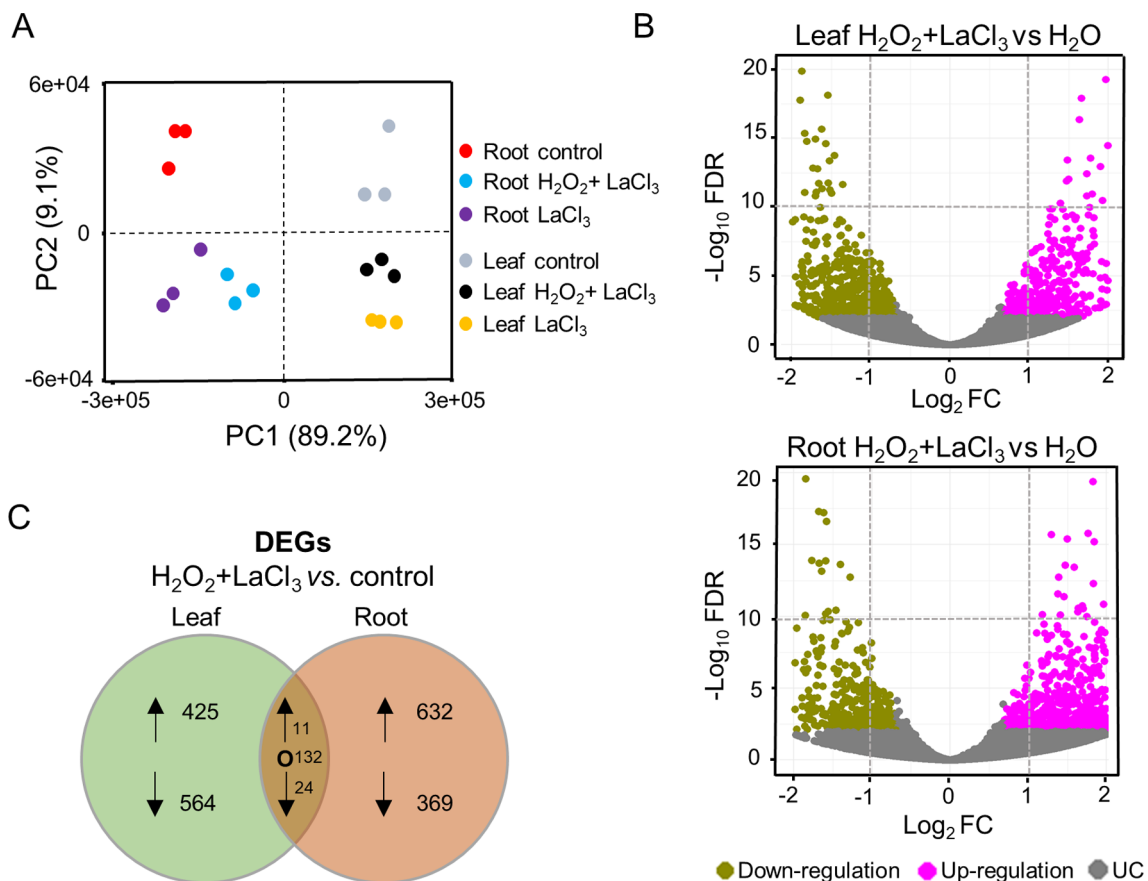


Fig. 2 Differentially expressed genes (DEGs) in H₂O₂ + LaCl₃ treated vs. control plants. **(A)** PCA plot illustrating the homogeneity of the gene counts obtained with the various treatments and tissues. PC1 (X-axis) separates the samples by tissue and PC2 (Y-axis) by treatment. **(B)** Volcano plots depicting DEGs obtained in leaves (upper panel) and roots (lower panel). The X-axis shows the fold change (log₂FC) and the Y-axis represents the statistical significance (-log₁₀FDR). DEGs (FDR < 0.01) are represented as up (magenta dots) and down (green dots) regulated, whereas genes with unchanged levels (UC) (FDR > 0.01) are indicated as grey dots. **(C)** Bubble charts representing the unique DEGs (FDR < 0.01, |log₂FC| ≥ 0.5) of leaves and roots, after omitting DEGs shared between the H₂O₂ + LaCl₃ and the LaCl₃ treatment. Genes found in both tissues are also indicated. Arrows indicate up (↑) and down (↓) regulation. O indicates unchanged expression

Identification of Ca²⁺-dependent H₂O₂-responsive genes in leaves and roots of barley

A previous transcriptome analysis of barley had shown that 1001 and 1883 genes in leaves and roots, respectively, were differentially expressed upon H₂O₂ treatment [55]. These H₂O₂-DEGs were selected based on $\log_2FC \geq 0.5$ and $FDR < 0.01$ and were obtained by RNA-seq of samples obtained under the same experimental conditions as in the current study. To identify those H₂O₂-DEGs that depend on the H₂O₂-induced Ca²⁺ signals for their differential regulation, a comparative analysis between the transcriptomes in response to H₂O₂ [previously published data, 55] and to H₂O₂ + LaCl₃ was performed. More precisely, we selected those DEGs from the H₂O₂ treatment that either showed an unchanged

expression (UCs) under H₂O₂ + LaCl₃ treatment or which were DEGs under both treatments but their expression level differed significantly ($\Delta\log_2FC \geq 1$; corresponding to a fold change difference ≥ 2) when H₂O₂ treatment was compared to H₂O₂ + LaCl₃ treatment (Fig. 3A). $\Delta\log_2FC$ thus represents the difference between \log_2FC s obtained under two conditions, i.e., H₂O₂ vs. H₂O and H₂O₂ + LaCl₃ vs. H₂O.

All in all, about 33% and 70% of the H₂O₂-responsive genes in leaves and roots, respectively, were considered as Ca²⁺-dependent H₂O₂-responsive genes in barley (Fig. 3B). Of those, 295 genes in leaves and 799 genes in roots showed a strict dependency (DEGs-H₂O₂ vs. UCs-H₂O₂ + LaCl₃) on Ca²⁺ signals (Fig. 3B; Table S3 and S4). 36 genes in leaves and 522 genes in roots were either

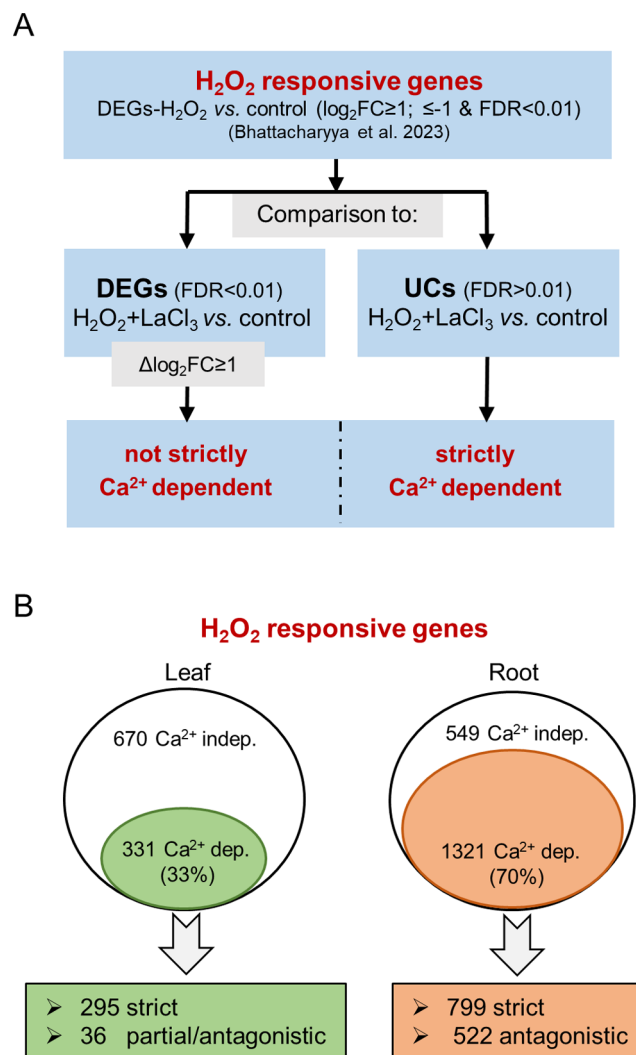


Fig. 3 Identification of Ca²⁺-dependent H₂O₂-responsive genes. **(A)** Schematic representation of the bioinformatic analysis steps to identify Ca²⁺ dependent H₂O₂-responsive genes in leaves and roots of barley. UCs: genes with unchanged expression between H₂O₂ + LaCl₃ and control. $\Delta\log_2FC$ represents the difference between \log_2FC s obtained under two conditions, i.e. H₂O₂ vs. control and H₂O₂ + LaCl₃ vs. control. **(B)** Egg-shaped representations of the comparison between Ca²⁺-dependent and Ca²⁺-independent H₂O₂-responsive genes in leaves and roots of barley. The Ca²⁺-dependent genes were further divided in strict and partial/antagonistic with regards to Ca²⁺

partially dependent on Ca^{2+} signals (altered up- or down-regulation levels), or even displayed a counter-regulation from up to down or vice versa.

GO analyses of Ca^{2+} -dependent H_2O_2 -responsive genes

GO enrichment analyses were performed with the obtained Ca^{2+} -dependent H_2O_2 -responsive genes in leaves and roots of barley (Fig. 4). In leaves, the top biological terms were related to jasmonate (JA) signaling and wounding. Further enrichment was observed for terms related to abiotic stresses in general and salt, osmotic stress, and temperature in particular. Further GO terms were related to hormones and oxygen-containing compounds (Fig. 4A). By contrast, the root gene set yielded mostly GO terms associated with ROS/ H_2O_2 response and metabolism, response to oxidative stress,

and detoxification but also to cell wall biogenesis and organisation (Fig. 4B).

Clustering analysis of Ca^{2+} -dependent H_2O_2 -responsive genes

Clustering analysis of the Ca^{2+} -dependent H_2O_2 -responsive genes provided five clusters, L1-L5, for leaves and four clusters, R1-R4, for roots (Fig. 5, Fig. S2). In leaves, cluster L1 and L2 comprise genes which were up- and down-regulated under H_2O_2 , respectively, however, in the presence of $\text{H}_2\text{O}_2 + \text{LaCl}_3$ their expression level was unchanged compared to control conditions (Fig. 5A, Table S3). This indicates a strict dependence of their response to H_2O_2 on Ca^{2+} signals. The genes in cluster L3 and L4 showed a reduced up- and down-regulation in response to H_2O_2 , respectively, when the Ca^{2+} transient

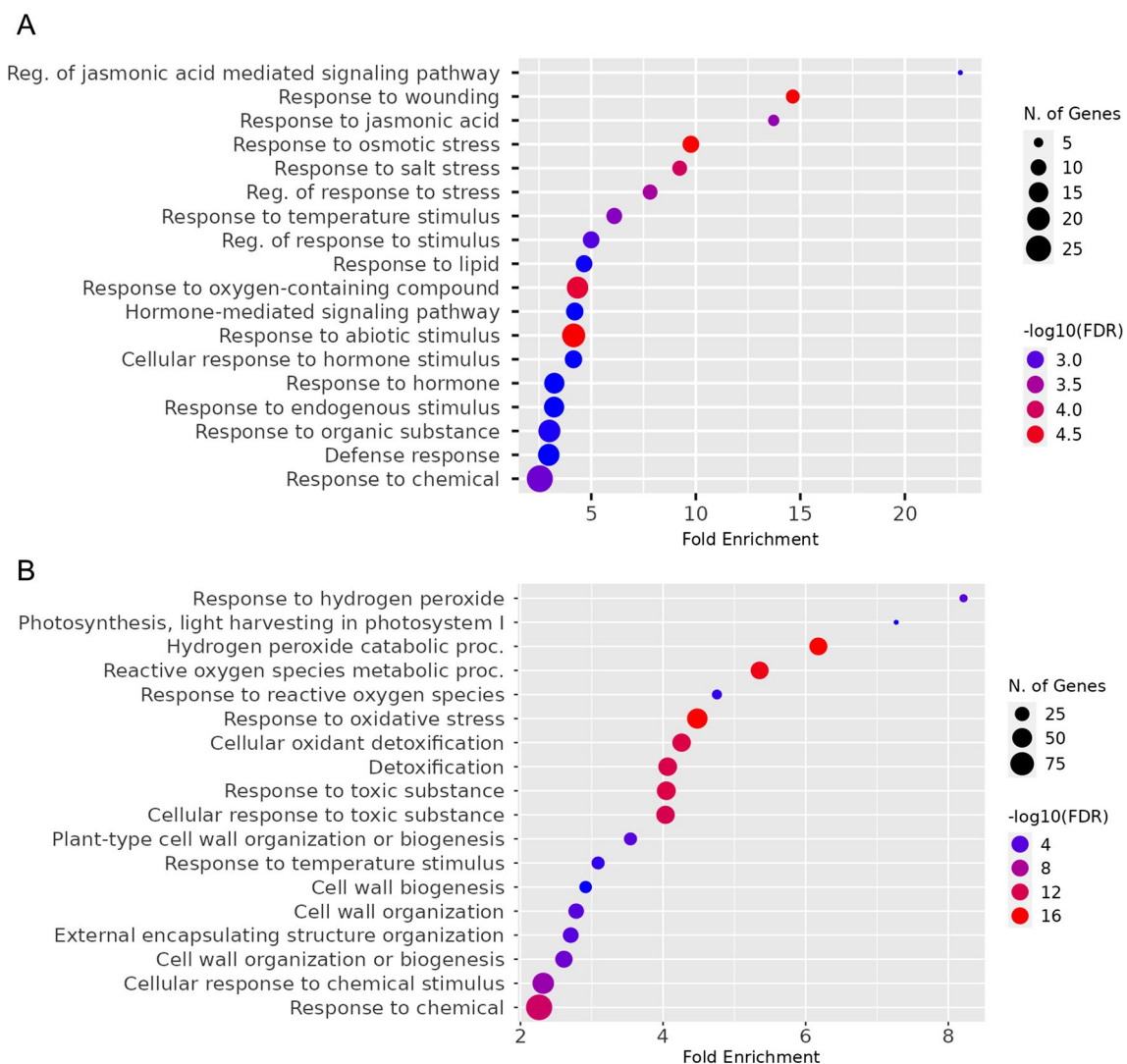


Fig. 4 Gene ontology enrichment analysis of Ca^{2+} -dependent H_2O_2 -responsive genes. The diagrams of enriched GO terms indicate total number of genes associated with various biological processes and their fold enrichment (relative to their overall occurrence in the genome) in (A) leaves and (B) roots of barley

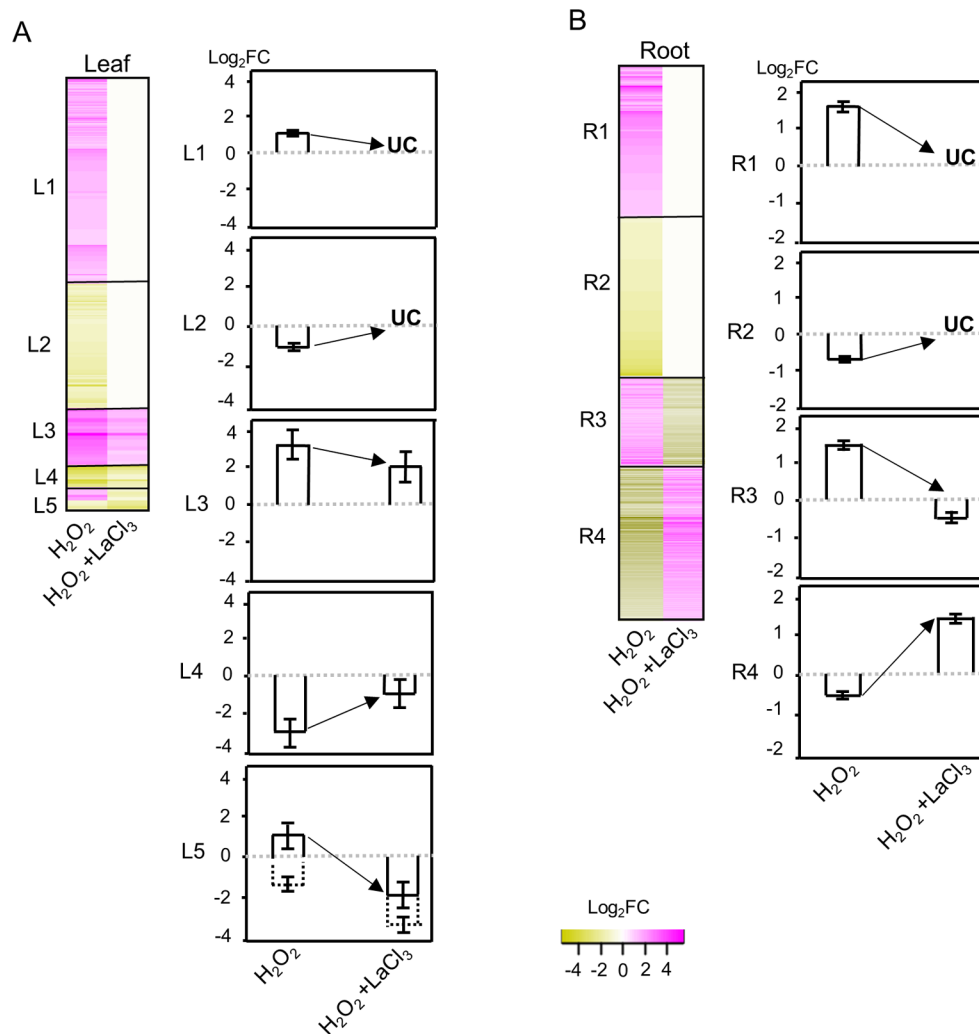


Fig. 5 Clustering analysis of the Ca²⁺-dependent H₂O₂-responsive genes. Gene clustering was used to group the Ca²⁺-dependent H₂O₂-responsive genes with similar expression patterns. The results provided five clusters in leaves (**A**) and four clusters in roots (**B**). Left panels of each subpart represent the heatmap of the genes in the clusters, and the right panel shows a bar chart representation of the mean \pm SE of the log₂FC of the genes in each cluster. UC: genes with unchanged expression between H₂O₂ + LaCl₃ and control

was blocked by LaCl₃, however, transcript levels were still significantly higher or lower compared to the control. Thus, cluster L3 and L4 represent H₂O₂-responsive genes with partial dependence on Ca²⁺. Cluster L5 contains H₂O₂-responsive genes that went from up- to down-regulation upon inhibition of the Ca²⁺ transient but also three genes for which their down-regulation was enhanced. Remarkably, in roots cluster R1 and R2 represent many genes with a strict dependence on the Ca²⁺ transient for their up- or down-regulation, respectively, however, in contrast to leaves, no partial up- and down-regulation was observed. Instead, clusters R3 and R4 comprise many H₂O₂-responsive genes which upon inhibition of the Ca²⁺ signal went from up- to down-regulation and vice versa (Fig. 5B, Table S4).

To verify the accuracy of the RNA-seq data and clustering analysis, the expression levels of two randomly

selected genes from each cluster were re-evaluated by RT-qPCR (Figs. 6 and 7). For all candidate genes tested, the transcript levels determined by RT-qPCR showed similar trends as observed in the RNA-seq data. Linear regression analysis showed a correlation coefficient of >0.7, indicating a positive correlation between RT-qPCR and RNA-seq data for all treatments and tissues (Fig. S3).

Cluster L1

Cluster L1 (up-regulation is strictly dependent on a Ca²⁺ signal) has a total of 196 genes, over 20 of which encode members of TF families (Table S3). Several of these TFs belong to the AP2/ERF (APETALA2/ethylene response factor) family, which has been associated with a wide variety of environmental stresses including hypoxia, cold, oxidative, and flooding stress not only in Arabidopsis but also in other plant species [72, 73]. Originally

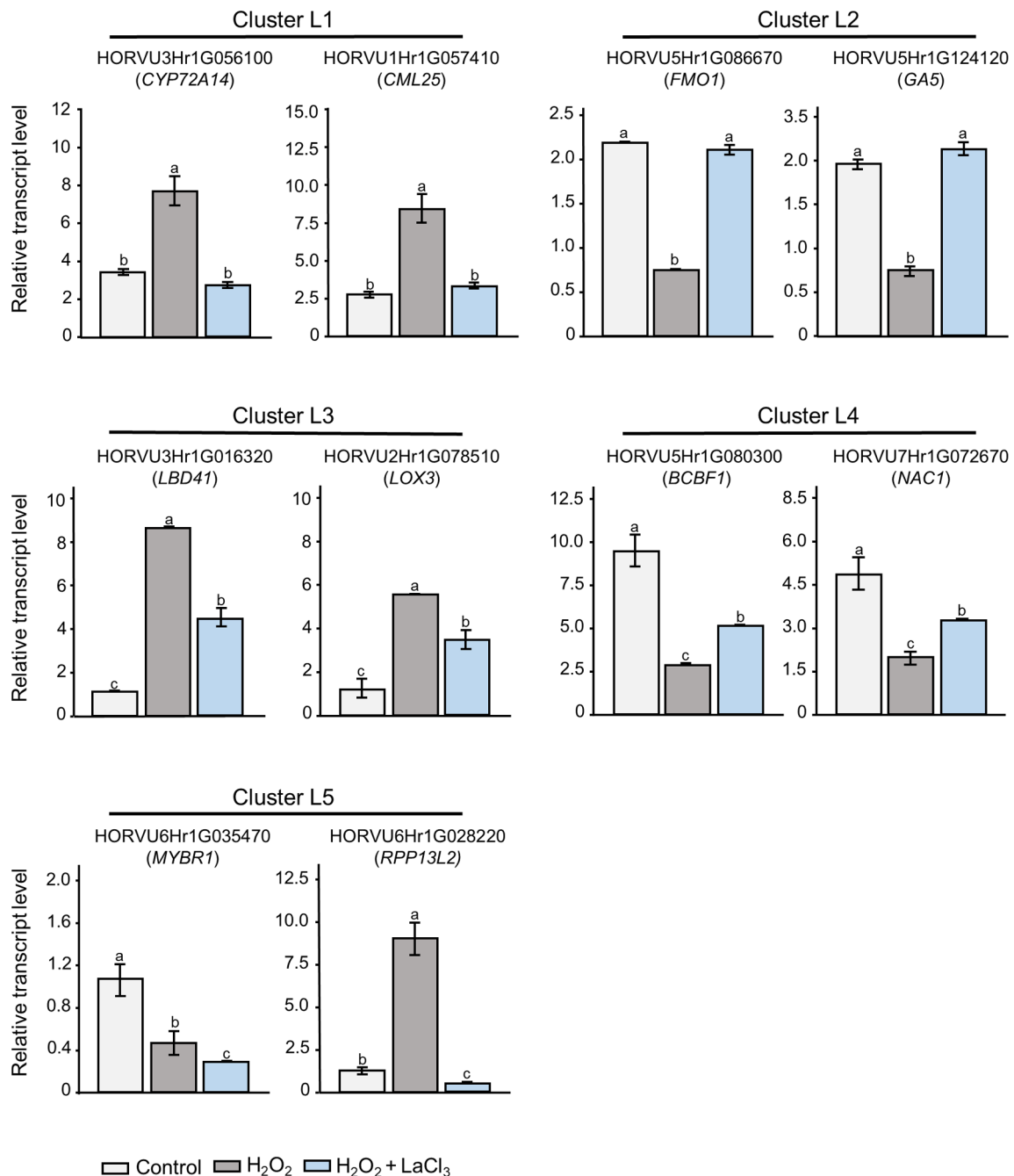


Fig. 6 RT-qPCR analyses of transcript levels in leaves. Two Ca²⁺-dependent H₂O₂-responsive genes from each leaf cluster were randomly selected. Data represent mean ± SE of three independent biological replicates and two technical repeats ($n=3$). The transcript levels were normalized to the reference genes *HvACTIN* and *HvGAPDH*. Statistical significances were obtained using one-way ANOVA and Tukey's Post-Hoc HSD test ($P < 0.05$). The letters represent different levels of significance. Orthologous genes in Arabidopsis are indicated in brackets

associated with ethylene signaling, AP2/ERF TFs have also been connected to other hormones like abscisic acid (ABA), gibberellic acid (GA), and cytokinin [74]. Genes associated with these hormones were also found in this cluster. Other important TFs in cluster L1 belong to the WRKY, NAC, and F-BOX domain-containing TF families. These TF families have been shown to function

ubiquitously in a variety of abiotic and biotic stimuli by intercepting the ROS signaling [75–77]. Cluster L1 furthermore contains several genes related to Ca²⁺ signaling such as orthologs of genes encoding the calmodulin-like proteins AtCML11, AtCML25, or OsCML26 (LOC_Os12g01400.1), as well as AtCIPK1 (CBL-interacting protein kinase 1). It furthermore includes genes coding

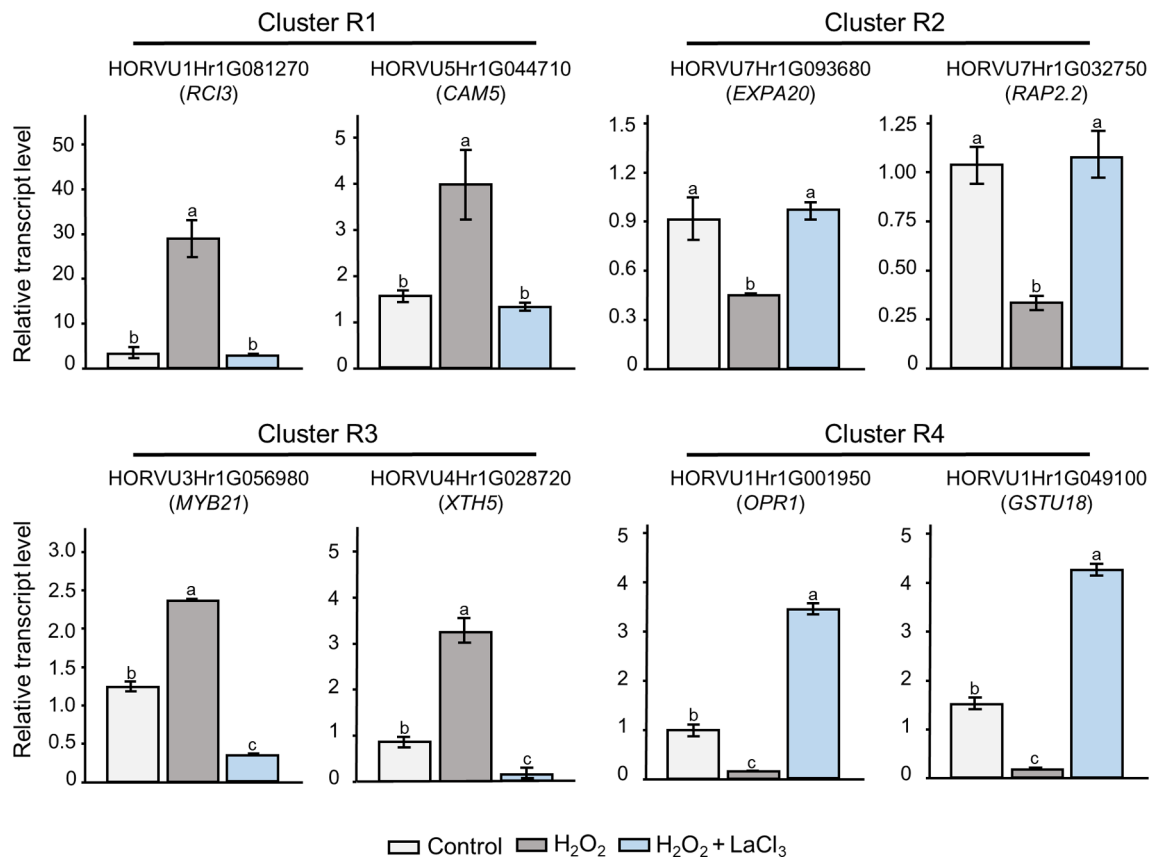


Fig. 7 RT-qPCR analyses of transcript levels in roots. Two Ca²⁺-dependent H₂O₂-responsive genes from each root cluster were randomly selected. Data represent mean ± SE of three independent biological replicates and two technical repeats (n=3). The transcript levels were normalized to the reference genes *HvACTIN* and *HvGAPDH*. Statistical significances were obtained using one-way ANOVA and Tukey's Post-Hoc HSD test ($P < 0.05$). The letters represent different levels of significance. Orthologous genes in Arabidopsis are indicated in brackets

for members of the MAPK (mitogen activated protein kinase) and MAPKKK (MAPK kinase kinase) family. With regard to hormone signaling, genes found in cluster L1 encode negative regulators of the JA pathway including proteins involved in the degradation of the biologically active form of jasmonate, JA-Ile [78, 79]. Genes encoding proteins involved in catabolic function were also found for GA, cytokinin and ABA. We furthermore identified three auxin responsive genes, only one of which has an ortholog in Arabidopsis (*AtIAA22*).

Cluster L2

Cluster L2 (down-regulation is strictly dependent on a Ca²⁺ signal) comprises a total of 99 genes. It also includes genes coding for various TFs of the AP2/ERF, WRKY, OVATE, or F-BOX families (Table S3). The AP2/ERF TFs were orthologs of *AtERF1* which has been associated with both JA and ethylene signaling [80], and *AtRAV2* which has been proposed to be involved in touch stimuli induced signaling [81]. Additionally, several genes encoding kinases associated with signal transduction events were identified including orthologs of the cysteine receptor kinase 28 (*AtCRK28*), which was associated with

ROS-related stress responses [82]. Cluster L2 includes three genes encoding class III plant peroxidases, particularly orthologs of *AtPRX52* and *AtPRX72* [83]. Interestingly, L2 was the only cluster in leaves that includes a group of genes encoding transport proteins, such as orthologs of the ABC domain containing JA/JA-Ile transporter *AtABCG16/JAT1* [84] and of AZA-RESISTANT GUANINE 2 (*AtAZG2*), a member of the AZG purine transporter family that has been shown to function in transportation of cytokinin [85]. Additionally, this cluster contains a number of other genes that play important roles in different stress pathways in plants such as orthologs of the *FLAVIN MONO-OXYGENASE 1 (AtFMO1)*, which is positioned downstream of SA induced Systemic Acquired Resistance (SAR) and related signaling pathways [86] and has also been associated with *AtCDPK5* a target of Ca²⁺ signals [87, 88].

Cluster L3

Cluster L3 (up-regulation is partially dependent on a Ca²⁺ signal) consists of 16 genes, most of which have no functional annotation and only six have a clear ortholog in Arabidopsis (Table S3). Of these genes, one encodes

an ortholog of the TF AtLBD41, a class IIA LBD protein that was previously identified in relation to low-oxygen endurance or high-light-induced increase in H₂O₂ in Arabidopsis [89, 90] as well as flooding response in soybean [91]. Another one encodes an ortholog of the 13 S-lipoxygenase 3 (AtLOX3), an enzymes that catalyze the first step in the biosynthesis of JA [92]. LOX3 was shown to play an important role in vegetative growth restriction after wounding [93], parasitic nematode infection [94], and salt stress [95], responses all of which include H₂O₂ and Ca²⁺ signaling.

Cluster L4

Cluster L4 (down-regulation is partially dependent on Ca²⁺ signal) comprises only 10 genes, Similar to cluster L3 many have no assigned function and only three have known orthologs in Arabidopsis (Table S4). Three TFs were found including HORVU3Hr1G010190, which is a different ortholog of AtRAV2 than the one found in cluster L2. Thus, RAV2-encoding genes show both strict and partial dependence on Ca²⁺ in their H₂O₂-induced down-regulation. In this cluster we also found the gene *HORVU1Hr1G063780*, which is an ortholog of *AtGA20OX2*, which plays an important role in the rate-limiting steps of GA biosynthesis [96]. The GA20 oxidases, *AtGA20OX1* and 2 are supposed to have a partially redundant function; however, we found the barley ortholog of *AtGA20OX1* within the up-regulated genes (in cluster L1).

Cluster L5

Cluster L5 combines genes with two different types of regulation pattern. Three of the 10 genes showed enhanced down-regulation when Ca²⁺ signals were inhibited by LaCl₃. The other seven displayed counter-regulation going from up-regulation by H₂O₂ to down-regulation under combined H₂O₂+LaCl₃ treatment. For only five genes an Arabidopsis ortholog and thus a potential function was identified (Table S3) and none of the genes in cluster L5 have so far been linked to H₂O₂ or Ca²⁺ signaling. One gene with enhanced down-regulation encodes an ortholog of AtMYBR1, also called MYB44, a TF that has been shown to negatively regulate ABA signaling by interacting with the nuclear ABA receptor PYR1-LIKE 8 [97]. It has also been associated with other hormone responses, i.e. to JA and SA [98].

Cluster L5 combines genes with two different types of regulation pattern. Three of the 10 genes showed enhanced down-regulation when Ca²⁺ signals were inhibited by LaCl₃. The other seven displayed counter-regulation going from up-regulation by H₂O₂ to down-regulation under combined H₂O₂+LaCl₃ treatment. For only five genes an Arabidopsis ortholog and thus a potential function was identified (Table S3) and none of

the genes in cluster L5 have so far been linked to H₂O₂ or Ca²⁺ signaling. One gene with enhanced down-regulation encodes an ortholog of AtMYBR1, also called MYB44, a TF that has been shown to negatively regulate ABA signaling by interacting with the nuclear ABA receptor PYR1-LIKE 8 [97]. It has also been associated with other hormone responses, i.e. to JA and SA [98].

Cluster L5 combines genes with two different types of regulation pattern. Three of the 10 genes showed enhanced down-regulation when Ca²⁺ signals were inhibited by LaCl₃. The other seven displayed counter-regulation going from up-regulation by H₂O₂ to down-regulation under combined H₂O₂+LaCl₃ treatment. For only five genes an Arabidopsis ortholog and thus a potential function was identified (Table S3) and none of the genes in cluster L5 have so far been linked to H₂O₂ or Ca²⁺ signaling. One gene with enhanced down-regulation encodes an ortholog of AtMYBR1, also called MYB44, a TF that has been shown to negatively regulate ABA signaling by interacting with the nuclear ABA receptor PYR1-LIKE 8 [97]. It has also been associated with other hormone responses, i.e. to JA and SA [98].

Cluster R1

Cluster R1 (up-regulation is strictly dependent on a Ca²⁺ signal) contains a total of 389 genes, including several TFs mostly belonging to sub-families like AP2/ERE, WRKY, MYB, OVATE, bHLH, HOMEBOX, F-BOX, GATA, and LEA (Table S4). Cluster R1 also contains genes encoding proteins related to glutathione metabolism and other forms of detoxification. By far the largest functional group are anti-oxidant enzymes with the majority being class III plant type peroxidases. Nine of these encode different barley orthologs of AtRCI3 and seven include orthologs to the secretory peroxidase AtPRX39 both of which has been associated with cold stress and tolerance [99, 100]. Also, genes related to Ca²⁺ signaling were identified such as orthologs of *AtCAM5* [101] and the Ca²⁺-dependent NADPH oxidase *RBOHD* [45, 102], *AtCPK5* [103], and *AtMPK9*, a MAP kinase shown to positively regulate ROS-mediated ABA signaling downstream of Ca²⁺ signals [104]. Other kinases include orthologs of the cytoplasmic histidine kinase *AtAHK5*, the mutation of which leads to reduced stomatal closure in response to H₂O₂ [105] The gene *HORVU5Hr1G046020* encodes an ortholog of *AtPBL8*, a member of the subfamily VII of receptor-like cytoplasmic kinases (RLCK), other members of which were found in all root clusters and in leaf clusters L1 and L2. Several RLCKs play a role in pattern-triggered immune signaling, and the higher order mutant *atpbl8/16/17* showed increased flg22-triggered H₂O₂ generation [106].

Cluster R2

Cluster R2 (down-regulation is strictly dependent on a Ca^{2+} signal) is the largest cluster with 410 genes (Table S4). Again, a number of TFs belonging to different families were found in this cluster, including an ortholog of *AtERF1*, albeit a different one to the ortholog found in cluster L2. Similar to cluster R1, this cluster also contains genes encoding proteins involved in ROS metabolism and detoxification, such as another ortholog of *AtPRX52*. The cluster R2 contains several genes coding for proteins with Ca^{2+} -binding EF-hand domains, one of them being an ortholog of *AtCML39*. Interestingly in this cluster we found six genes related to photosynthesis, encoding orthologs of the Arabidopsis chlorophyll-binding proteins of the LHCA and LHCB type as well as *AtPSB28* and *AtPSAK*. Cluster R2 also comprises orthologs of several genes involved in hormonal signaling.

Cluster R3

Cluster R3 (counter-regulation from up to down) contains 128 genes. As in most clusters, we found genes belonging to major TF families (Table S4). We also found two peroxidases, orthologous of Arabidopsis *AtPRX71* and *AtRCI3*, the ortholog of TPR like thioredoxin *AtTTL1*, and genes associated with various aspects of hormone signaling. Additionally, several components of Ca^{2+} signaling pathways were present in this cluster such as orthologs of the Ca^{2+} sensor *AtCML25* and the Ca^{2+} associated protein kinases *AtCPK13*.

Cluster R4

Cluster R4 (counter-regulation from down to up) contains in total 394 genes, again with several members of different TF families (Table S4). Interestingly, this cluster contains an ortholog of vascular plant one-zinc finger 1 (*AtVOZ1*), which has been implicated in heat stress response in plants and acting as a repressor of *DREB2C* [107]. Cluster R4 also encompasses genes related to glutathione metabolism and detoxification, including four orthologs of the glutathione transferase *AtGSTU18*, for which orthologs were also found in cluster L2 and R2, and three for *AtGSTF13*. Many genes encoding for phi (GSTF) and tau (GSTU) glutathione transferases are upregulated under environmental stress and Arabidopsis plants overexpressing *VvGSTU13* showed enhanced tolerance to a variety of abiotic stress conditions like cold and salt [108]. This cluster contains further anti-oxidant enzymes, including three orthologs of *AtPRX52*, all of them encoded by barley paralogs different from those present in clusters L2, R1, and R2. Cluster R4 exhibits the largest number of HSPs, most of which were small HSPs (SHSPs) as well as HSPs mapping to the Arabidopsis orthologs *AtHSP81-1*, *AtHSP101*, and *AtHSP70*. Also in this cluster we found 14 genes related to photosynthesis.

Transcription factors as key regulators of Ca^{2+} -dependent H_2O_2 -responsive genes in barley

We next modelled potential connections from known components of Ca^{2+} signaling networks to the identified Ca^{2+} -dependent H_2O_2 -responsive genes (Fig. S4) using CKN of the recently described SKM resource [65]. The information in the CKN is based on present knowledge from Arabidopsis, thus only 192 and 894 Ca^{2+} -dependent H_2O_2 -responsive genes found in leaves and roots of barley, respectively, with identifiable orthologs in Arabidopsis were considered for analysis (Tables S3 and S4). We extracted the directed shortest paths from known Ca^{2+} signaling related genes (source set) to the Ca^{2+} -dependent H_2O_2 -responsive genes identified in our transcriptomic analysis (target set). We additionally required that the final edge regulating the target gene was a transcriptional regulatory interaction. Merging of the results revealed several major network hubs connecting multiple Ca^{2+} signaling components to multiple targets in leaves and roots (Figs. 8A and 9A). The most dominant of these hubs (by number of times they occur in a path as well as number of targets) were depicted separately (Figs. 8B-E and 9B-E). In both, leaves and roots these hubs were defined by the TFs *AGL15*, *HY5*, *PIF4*, and *EIN3* as key nodes regulating several targets (Figs. 8 and 9, orange nodes). The Ca^{2+} signaling components in these networks were mostly CaMs/CMLs and CDPKs/CPKs but also CaM-interacting proteins such as IQD6.

Ethylene insensitive 3 (*EIN3*)

Downstream of *EIN3*, the targets in both tissues include a unique mosaic of genes from different signaling pathways (Figs. 8B and 9B), with a greater prevalence of genes from cluster L1 in leaves (strict positive dependence on cytosolic Ca^{2+} signals) whereas in roots the target genes were interspersed from all the clusters. Noteworthy is the *ERF1* gene, encoding an AP2/ERF transcription factor, which is present in our data as a down-stream target of *EIN3* in both tissues (Figs. 8B and 9B). This is in line with a previous study that identified *ERF1* as a downstream component of the ethylene signaling pathway, whose expression is regulated by *EIN3* binding to the *ERF1* promoter in vivo [109]. *ERF1* was shown to integrate JA and ethylene signalling pathways in a synergistic manner during plant defense [80] This crosstalk fits to other *EIN3*-regulated targets found in our dataset such as the JA catabolic protein *CYP94C1* and the ethylene biosynthetic protein 1-aminocyclopropane 1-carboxylate oxidase 5 (*ACO5*), which is known to have *EIN3* binding sites [110].

Hypocotyl 5 (*HY5*)

All downstream targets of *HY5* in leaves belong to cluster L1 (Fig. 8C), thereby suggesting a pre-dominant strict

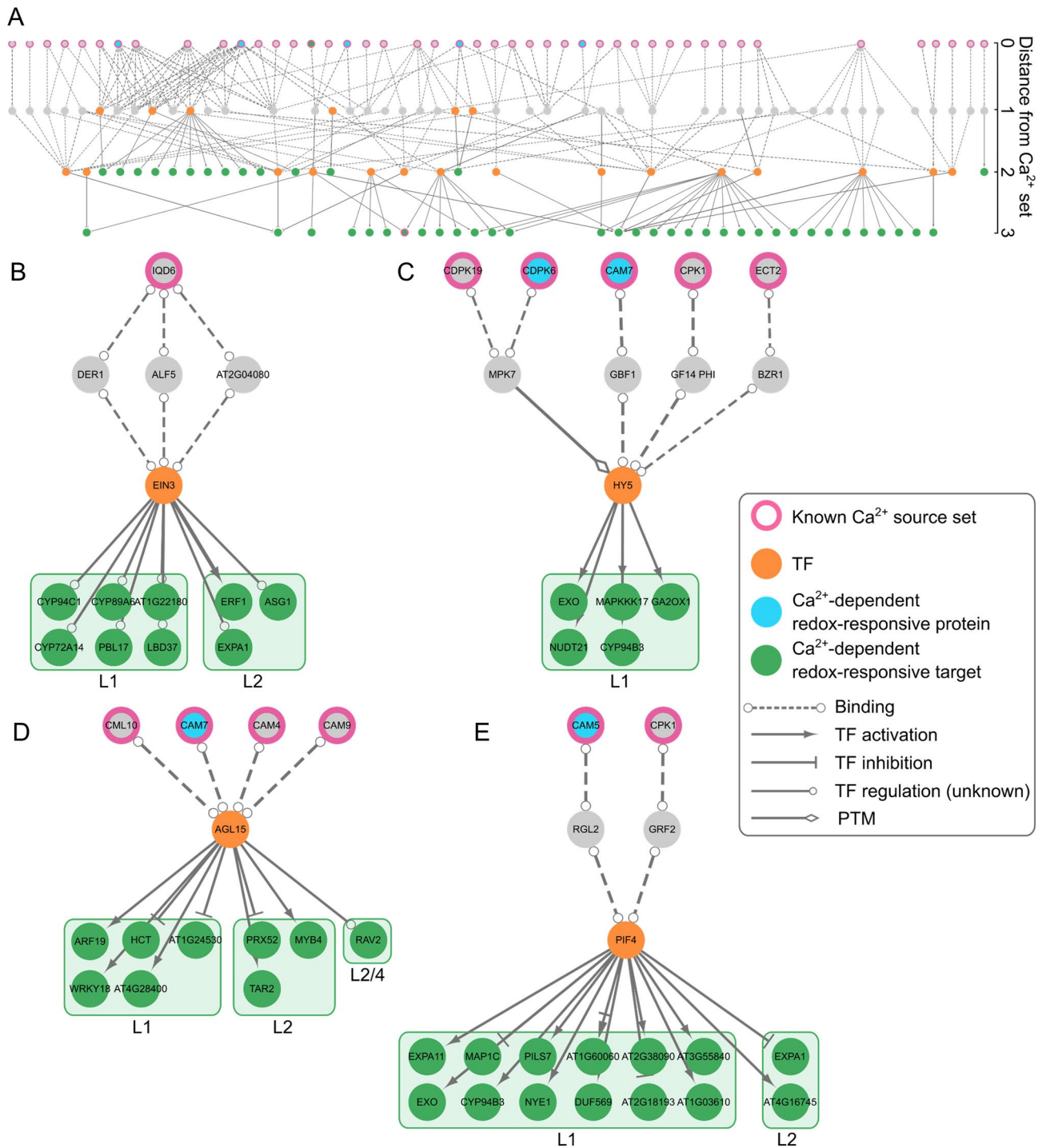


Fig. 8 Network analyses of Arabidopsis orthologs of the Ca²⁺-dependent H₂O₂-responsive genes found in barley leaves. **(A)** All shortest paths identified in KGN starting from known Ca²⁺-related genes (sources, pink-bordered nodes) to Ca²⁺-dependent H₂O₂-responsive genes identified by RNA-seq (targets, green-filled nodes) merged into a single network. Sub-networks were extracted from the merged network with focus on **(B)** EIN3, **(C)** HY5, **(D)** AGL15 and **(E)** PIF4. Ca²⁺-related components identified in a previous proteomic study as H₂O₂-regulated in Arabidopsis leaves [65] are presented by a light blue-filling. Nodes are labelled with their short names, when available. The targets are ordered by corresponding clusters (L). PTM: post-translational modification, TF: transcription factor. Complete networks are provided in additional file 1

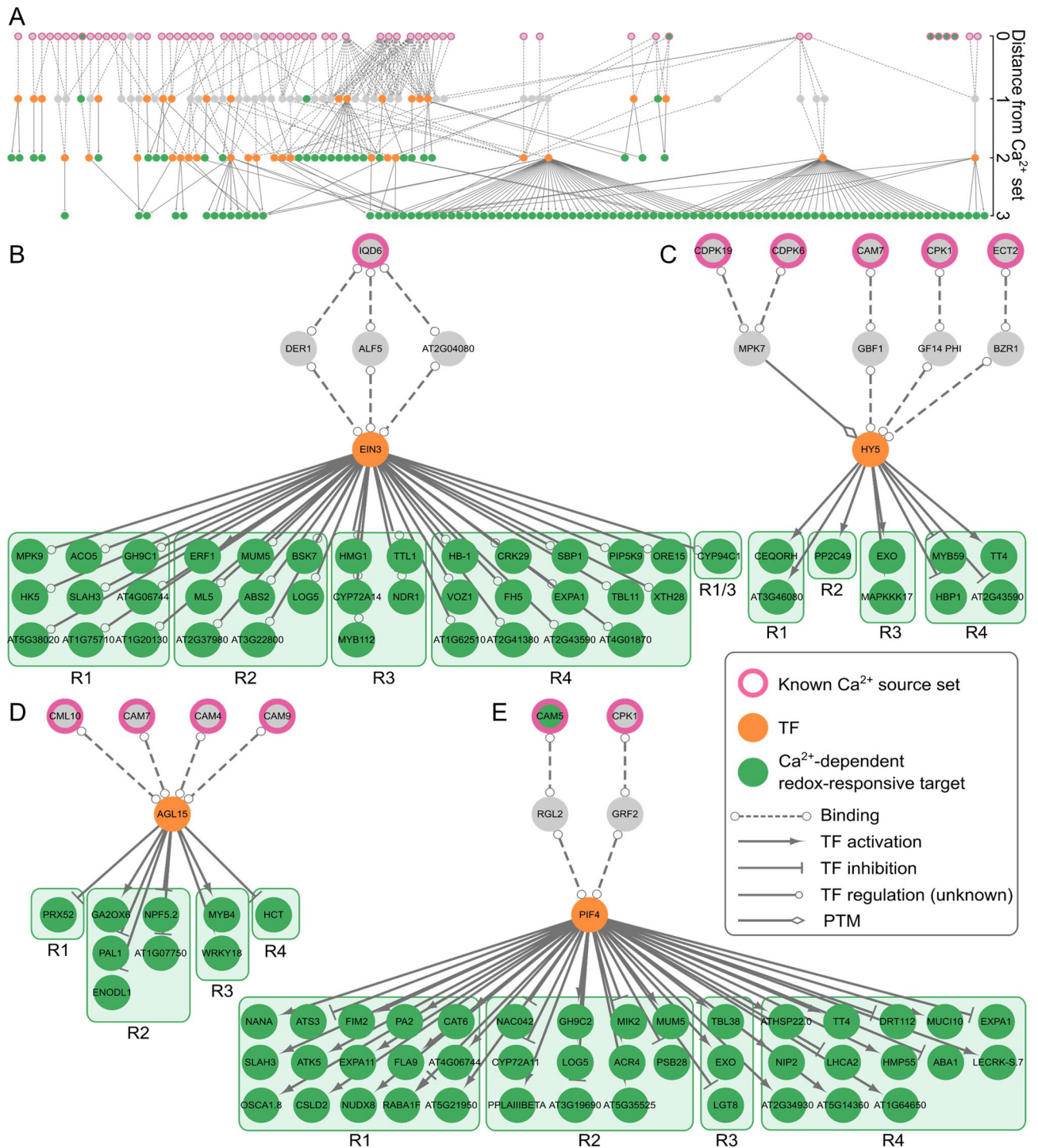


Fig. 9 Network analyses of Arabidopsis orthologs of the Ca²⁺-dependent H₂O₂-responsive genes found in barley roots. **(A)** All shortest paths identified in CKN starting from known Ca²⁺-related genes. (sources, pink-bordered nodes) to Ca²⁺-dependent H₂O₂-responsive genes identified by RNA-seq (targets, green-filled nodes) merged into a single network. Sub-networks were extracted from the merged network with focus on **(B)** EIN3, **(C)** HY5, **(D)** AGL15 and **(E)** PIF4. Nodes are labelled with their short names, when available. The targets are ordered by corresponding clusters (R). PTM: post-translational modification, TF: transcription factor. Complete networks are provided in additional file 1

dependency on Ca^{2+} signals for up-regulation, while in roots this TF again had downstream targets in all clusters (Fig. 9C). The targets in leaves include genes like the MAPKK kinase *MAPKKK17*, involved in plant herbivory responses [111], the phosphatase *PP2C49*, a negative regulator of salt stress tolerance in *Arabidopsis* [112], the *ceQORH* protein, a long-chain fatty acid reductase whose allocation between cytosol and chloroplasts is depending on CaM-binding [113], and the TF *MYB59* already established in negative regulation of Ca^{2+} signaling and homeostasis [114]. *HY5* is known to play a role in plant thermomorphogenesis in coordination with another TF, *PIF4* [115], which is also present in our network as a nodal hub (see below).

Agamous like 15 (AGL15)

Again, the largest group of *AGL15* downstream targets in leaves include genes from cluster L1 and L2 (Fig. 8C), representing a strict dependence on Ca^{2+} signals. In roots, the targets of *AGL15* include mostly genes from cluster R2 (Fig. 9C), thereby also showing strict dependency on Ca^{2+} . Common between leaf and root targets is the TF *MYB4*, which has an established role in protection against oxidative stress during cadmium stress [116] and flavonoid biosynthesis [117]. The targets also include an ortholog of the peroxidase *PRX52*, which has a number of orthologs in barley and is present in different clusters.

Phytochrome interacting factor 4 (PIF4)

The downstream targets of *PIF4*, also called *SRL2*, in leaves include mostly genes from cluster L1 (strict dependence on Ca^{2+} signals for H_2O_2 induced up-regulation), most of them without a direct relationship to ROS, Ca^{2+} signalling or stress. In roots, downstream targets were found in all clusters and included genes encoding for the Ca^{2+} channel *OSCA1.8* involved in osmotic stress induced Ca^{2+} signatures [118], the RAB GTPase *RABA1f* involved in salt stress response [119], and the TF *NAC042* previously shown to be involved in salt and drought stress [120, 121]. Furthermore, targets of *PIF4* include genes coding for proteins involved in detoxification of ROS.

Discussion

Our comparative analysis between the already published transcriptome changes induced by H_2O_2 [55] and those observed under a combined application of $\text{H}_2\text{O}_2 + \text{LaCl}_3$ (this study) showed that the H_2O_2 -induced Ca^{2+} signals affected the transcript abundance of many H_2O_2 -responsive genes. The transcriptome changes were not due to an interference with Ca^{2+} homeostasis per se, since only those genes from the $\text{H}_2\text{O}_2 + \text{LaCl}_3$ set that displayed changes under H_2O_2 alone but no changes with LaCl_3 alone were considered. Overall, in roots more

H_2O_2 -responsive genes showed a dependency on the H_2O_2 -induced Ca^{2+} signals compared to those in leaves (Fig. 3). This is in line with the higher number of genes for which transcriptional changes were observed after H_2O_2 treatment alone in roots [55]. However, even considering these differences in total numbers, expression of only 33% of the H_2O_2 -responsive genes in leaves, but about 70% of those in roots, was affected by LaCl_3 -sensitive Ca^{2+} signals (Fig. 3B). Moreover, most of the identified Ca^{2+} -dependent H_2O_2 -responsive genes were found only in one of the two tissues, indicating a clear tissue specificity of the response. H_2O_2 is not only generated in response to biotic attacks but also by imbalances in energy metabolism. Obviously, photosynthesis is a process generating a large amount of ROS and thus, leaf tissue simply might have a higher prevalence of detoxification systems already in place while they need to be induced upon the accumulation of H_2O_2 in roots. This would be in line with the observation that many genes related to oxidative stress and detoxification were observed in response to H_2O_2 in roots [55]. We also observed minor differences in H_2O_2 penetration (Fig. 1B) and a slightly stronger inhibition of the Ca^{2+} signal (Fig. 1C) by LaCl_3 in roots which might further affect the transcriptome changes.

The issues discussed above notwithstanding, strict and partial/antagonistic Ca^{2+} dependency of the H_2O_2 -responsive transcriptome was observed in both tissues (Figs. 3 and 5). Strict dependency (clusters L1, L2, R1, and R2) means that genes with significant changes in transcript level upon H_2O_2 application no longer showed significant changes after LaCl_3 pre-incubation when compared to the control. The most likely scenario for these genes is that a Ca^{2+} signal evoked by H_2O_2 is required to activate a transcription activator or repressor (Fig. 10, strictly). This can occur either more directly, e.g., by proteins such as Ca^{2+} -dependent TFs or CAM-TAs [122], or as the consequence of a longer signalling cascade that involves Ca^{2+} activated proteins such as CDPKs, CaMs, or CBLs [123, 124]. Such strictly Ca^{2+} -dependent H_2O_2 -responsive genes were strongly dominant in leaves (~90%) and also the majority in roots (~60%). Partially dependent genes showed a difference in transcript abundance between control and $\text{H}_2\text{O}_2 + \text{LaCl}_3$ treatment; however, the abundance was significantly different from H_2O_2 treatment alone. Of these cases, genes in cluster L3 showed a reduced up-regulation in the absence of an H_2O_2 -induced Ca^{2+} transient, while genes in cluster L4 show reduced down-regulation (Fig. 10, additive). Interestingly, this kind of additive regulation of H_2O_2 and Ca^{2+} was completely absent in roots. For genes in these clusters H_2O_2 affects changes in transcript abundance both independently and via a Ca^{2+} signal, and both regulations occur in the same direction. Even in the absence of the H_2O_2 -induced Ca^{2+} transient, the direct

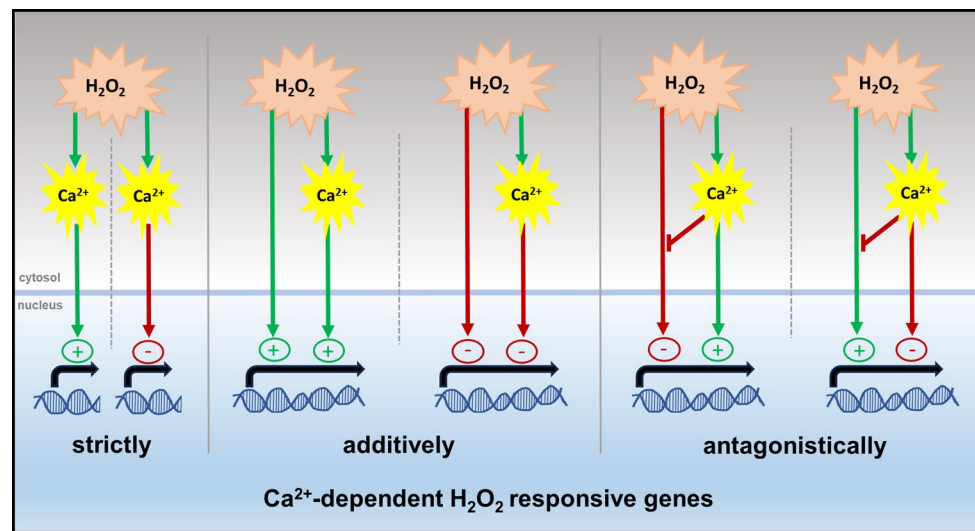


Fig. 10 Representative models of Ca²⁺-dependent H₂O₂-responses. Strict Ca²⁺-dependency means that Ca²⁺ signaling operates down-stream of H₂O₂ to induce either activation or repression of gene expression. Partial dependency is seen when H₂O₂ and Ca²⁺ signals modulate gene expression in an additive way. In that case, the H₂O₂ activation/repression of gene expression is not fully dependent on the H₂O₂-induced Ca²⁺ transient, but Ca²⁺ amplifies this regulation. In the antagonistic model, the H₂O₂-induced Ca²⁺ transient inhibits the H₂O₂-induced activation/repression while at the same time inducing an opposite response. Lack of the H₂O₂-induced Ca²⁺ transient thus results in a changes of transcript abundance from up to down and vice versa. The arrowheads indicate activation (green) or repression (red) and the red T-headed arrows indicate inhibition

regulation by H₂O₂ remains. More complex is the regulation of those genes from cluster L5, R3, and R4, for which inhibition of the H₂O₂-induced Ca²⁺ transient results in changes of transcript abundance from up to down and vice versa. The regulation of these genes can be explained by an antagonistic model (Fig. 10, antagonistic), where Ca²⁺-dependent and independent pathways act in the opposite direction and Ca²⁺ signaling in addition inhibits or attenuates the Ca²⁺-independent H₂O₂ induced activation/repression. Similarly, three genes in cluster L5 that show an increased reduction in transcript abundance in the absence of the Ca²⁺ transient could be regulated by multiple pathways in a Ca²⁺-dependent and -independent manner; however, in this case Ca²⁺ signaling attenuates the H₂O₂ response, so that it becomes stronger in its absence (Fig. S5). It should be noted that for all clusters more complex models can be envisioned. Also, transcript abundance is not necessarily defined by gene expression, however, the models can easily be adapted for changes in transcript stability or degradation.

Indeed, our results reinforce the notion of complex, interacting pathways that define the ultimate response to a certain stimulus. While the responses are specific with regards to many factors such as type of stimulus, timing, tissue or developmental stage, they are variances of very similar patterns. After stimuli perception, the information is forwarded through the cell by signaling cascades involving components such as secondary metabolites, ions like Ca²⁺, hormones, kinases, etc., to ultimately affect gene transcription, translation and/or protein activity. The latter is either due to novel synthesis, degradation or

alteration of activity that catalyses the molecular changes required. This cascade of event allows for multiple points of regulation and ensures a cross-talk of signals coming from different internal and external stimuli. Many of the intermediate players will be ready and in place to receive a stimulus; nevertheless, stimulus-induced transcriptional regulation of sensors, signaling kinases or TFs can occur to enhance the response or to initiate priming and long-term adaptation. Thus, it is not surprising, that TFs were found in all clusters. It is not uncommon to have TF cascades, in which an initially activated TF affects the transcription of multiple other TFs [125]. Also, different stresses can lead to binding of the target from TFs of different gene families to induce or repress the expression, e.g. the redox-related LEA protein *SAG21* binding to ERF (pathogen stress), WRKY (H₂O₂ stress), and NAC (wounding stress) TF [126].

Phytohormones have been repeatedly demonstrated to interact with each other at various points through versatile TF families, thereby eliciting a common, synchronized, and holistic change in the molecular and biochemical landscape of the plant in response to diverse stimuli [127]. Moreover, the study of interactions between phytohormones and secondary messengers like Ca²⁺ has gained momentum over the years; particularly the CDPKs have been closely linked to phytohormones such as GA, ABA, or JA in regulating crucial plant processes related to growth and development, flowering, and also responses and acclimation to a variety of biotic and abiotic stresses [128]. Other kinases, such as RLKs, were proposed to play crucial roles during growth-defense

trade-off, i.e. by intermingling with different phytohormone signal transduction pathways [129]. The presence of these kinases in different clusters is thus in line with a differential regulation through Ca^{2+} signals, but also suggest them as potential hubs which have the potential to transduce downstream signals crucial to the H_2O_2 - Ca^{2+} crosstalk by interacting with other major signaling pathways like phytohormones.

There are several remarkable differences between the response of leaves and roots. In general, the roots show a higher variety of GO terms compared to leaves (Tables S3 and S4). As mentioned above, roots show more changes in genes related to oxidative stress and detoxification. This is marked by a strong Ca^{2+} -dependent regulation of class III peroxidases with a total of 42 peroxidases present across all clusters. Also genes belonging to the GO term cell wall are more abundant in roots compared to leaves. Cell wall metabolism plays important roles in shaping plant responses to stress acclimation [130]. Several reactions associated with crosslinking of cell wall components, like hemicellulose and xyloglucans, along with crucial processes, like polymerization and depolymerization of cell walls, have previously been related to ROS production and anti-oxidant enzyme activities, which is a characteristic feature when plants are challenged with abiotic stress conditions [131]. For instance, the transcription factor short root (SHR) is involved in plant organogenesis including periclinal division in the root cortex that depends on an optimal H_2O_2 balance. On one hand, SHR activates H_2O_2 production by RBOHs and on the other hand induces SA signaling that increases H_2O_2 levels by repressing CATALASE 2 [132].

In roots, we also found a much larger and diverse group of membrane transporters as in leaves, i.e. the wall-associated-transporter-1-like (WAT1) and SWEET-type transporters, but also aquaporins. Aquaporins have been shown to be involved in dynamic ROS changes under stresses [133] and WAT1 was identified as a downstream target of RBOH-mediated ROS generation during parasitic infections [134]. More surprisingly, we could identify 20 genes involved in photosynthesis including LHC proteins and photosystems components to be regulated by H_2O_2 -induced Ca^{2+} signals in roots. The presence of photosynthesis-related genes in roots might seem a controversial result, but it could be hypothesized that the exposure of the roots to light for five days lead to such a phenomenon. Moreover, it was also proposed that root plastids might be involved in the process of anti-oxidative damage control under stress conditions which generate oxidative bursts [135, 136]. This has also been suggested in another study based on fluorescence spectra of Arabidopsis roots that showed a capacity of root plastids to form larger antenna complexes [137]. Our results therefore might point to a crucial and “less-known” role played

by the H_2O_2 - Ca^{2+} crosstalk in the induction of LHC-encoding genes and other genes related to photosynthesis in roots.

In an attempt to decipher the molecular basis of the Ca^{2+} -dependency of the H_2O_2 -induced transcriptional responses, we modelled potential connections between known components of the Ca^{2+} -signaling network and the Ca^{2+} -dependent H_2O_2 -responsive genes identified in this study. The Ca^{2+} -signaling components in this network included many CaMs, CMLs, and CDPKs, several of which, had been shown in a recent study in Arabidopsis leaves to undergo Ca^{2+} -dependent changes in protein level upon H_2O_2 application [65] (Fig. 8, light blue nodes). Moreover, the network analyses showed TFs, especially EIN3, AGL15, PIF4, and HY5, downstream of the Ca^{2+} components as hubs/nodal points regulating multiple Ca^{2+} -dependent H_2O_2 -responsive genes in different clusters in leaves and roots of barley (Figs. 8 and 9). These TFs are known from Arabidopsis to be involved in different physiological and developmental processes including phytohormone signaling and catabolism, photosynthesis, detoxification, cell wall metabolism, and cellular transport. EIN3 is a positive downstream regulator of the ethylene signalling pathway that affects various facets of plant development, several stress responses, and phytohormone pathways [138]. So far, ethylene signaling involving EIN3 has been related to Ca^{2+} and H_2O_2 during salt stress response in Arabidopsis [139]. According to our model, this H_2O_2 - Ca^{2+} regulation might be mediated by the CaM-binding protein IQD6 (IQ67 Domain Containing 6) (Figs. 8B and 9B), which is known to play a crucial role in plant growth and development [140]. HY5 is a bZIP type master transcriptional regulator of photomorphogenesis, also shown to be involved in other processes such as response to abiotic stresses [141]. It was also shown that HY5 participates in ROS homeostasis [142, 143] and to interact with CAM7 to regulate Ca^{2+} -dependent photomorphogenesis in plants [144]. Indeed, in our network CAM7 is connected to HY5 via the G-box-binding factor GBF1 (Figs. 8C and 9C), which was shown to play a role in plant defense upstream of SA [145]. We also obtained a connection with CDPK7 and MPK7, which possibly regulate HY5 expression through post-translational modifications. H_2O_2 was also shown to directly increase kinase activity of MPK7, underscoring the complexity of the signaling cross-talk [146]. AGL15 is a member of the MADS box TF family and was shown in vitro to bind CaM [147]. This is in line with our network analyses suggesting connections between AGL15 and multiple CaMs as well as CML10 (Figs. 8D and 9D). As for HY5, AGL15 regulation might also be controlled by CAM7.

PIF4, a member of the bHLH TFs family, has so far very little association with Ca^{2+} and ROS signaling, although

a recent report showed a connection to RBOHD-mediated up-regulation under salt stress [148]. RBOH is not present in our model since it was only shown that *PIF4* expression is attenuated in a *rboh* mutant. However, our model suggests regulation of *PIF4* by *CAM5* and *CPK1*, which have never been shown to be involved in any stress signaling pathways. Downstream, *CAM5* and *CPK1* were connected to *RGL2* (RGA-Like2), which is a member of the DELLA protein family and has previously been shown to be involved in ROS generation and phytohormonal signaling [149–151]. *GRF2* is a member of the 14-3-3 protein family. Although specific data linking *GRF2* to signaling or stress pathways is missing, 14-3-3 proteins have been previously linked to plant stress, Ca^{2+} signaling, and hormone signal transduction [152, 153].

However, it should be noted that the information in CKN used for our network modelling is based on current knowledge from Arabidopsis, so only those barley Ca^{2+} -dependent H_2O_2 -responsive genes with identifiable orthologs in Arabidopsis were considered for analyses. Thus, of the 331 and 1334 Ca^{2+} -dependent H_2O_2 -responsive genes in leaves and roots of barley, respectively, only 192 and 894 genes were used in CKN analyses. This clearly reinforces that there is an urgent need for more experimental data to be obtained from barley and other crops to close this vast knowledge gap. While multiple responses are conserved between different land plants, others are more specific. We will need to know the specific responses of crops for accurate stress for modeling and to use this information for improved crop breeding.

Conclusion

H_2O_2 is an indispensable ROS, which is generated as a toxic by-product of biological metabolic processes, but also functions as a signaling molecule that can influence plant growth and development. Moreover, it has an established potential to intermingle with signaling cascades associated with second messengers like Ca^{2+} . In this study, using transcriptomic analysis, the molecular landscape behind the tissue-wide H_2O_2 - Ca^{2+} crosstalk in the crop species barley was elucidated. Our data expands the knowledge on stress response in barley but also strengthen the relevance of findings in model plants such as Arabidopsis for barley. They reveal genes which have never been implicated in any canonical stress response pathway, and therefore may be used as candidates in future studies to further expand our understanding of this crosstalk. Similarly, network analyses suggested nodal TFs which in turn regulate the expression of genes involved in phytohormone pathways including ethylene, JA, ABA, SA, brassinosteroids, GA, and auxin, as well as in MAPK signaling cascades. Several studies have reported that both, biotic and abiotic stress, can lead to the accumulation of H_2O_2 and fluctuations in Ca^{2+} levels

which imply an enhancement in the vitality of plants to withstand those environmental stress. Hence, deciphering the molecular mechanisms underlying the H_2O_2 - Ca^{2+} crosstalk will ultimately provide more understanding of stress acclimation not only in barley but also in other crop species.

Supplementary Information

The online version contains supplementary material available at <https://doi.org/10.1186/s12870-025-06248-9>.

Supplementary Material 1: **Additional File 1:** Raw cytoscape output sessions (.cys) of the SKM network analyses in the roots and leaves of barley. Figures 8, 9 and S5 were prepared from the cytoscape files

Supplementary Material 2: **Additional File 2: Fig. S1** Unique and overlapping DEGs between $\text{H}_2\text{O}_2 + \text{LaCl}_3$ and LaCl_3 treatment alone vs. control treatment. Venn diagram of DEGs (FDR < 0.01) from (A) leaves and (B) roots. Only the unique DEGs from the $\text{H}_2\text{O}_2 + \text{LaCl}_3$ treatment were used for further analyses. **Fig. S2** Determining the number of clusters for Ca^{2+} -dependent H_2O_2 -responsive genes in (A) leaves and (B) roots. Gap statistics analysis was used for the calculation, with a total of 100 iterations. `set.seed(123)` function was used before running this function to reduce randomness and inconsistencies in the number of clusters generated. The number of clusters predicted by this analysis was used to perform k-means clustering analyses in figure 5. **Fig. S3** Validation of RNA-seq results by RT-qPCR. Linear regression analysis between transcript level ratios derived from RNA-seq and RT-qPCR data under different treatments in leaves (A and B) and roots (C and D). C: correlation coefficient, P: P-value, R2: R-regression coefficient. **Fig. S4** CKN analysis of H_2O_2 signaling based on Arabidopsis orthologs of the genes identified in barley. All paths identified in CKN leading from known Ca^{2+} -involved genes (pink-bordered nodes) to Ca^{2+} -dependent H_2O_2 responsive genes (green nodes), and from known redox-related genes (blue-bordered nodes) to Ca^{2+} -independent H_2O_2 -responsive genes (yellow nodes), obtained by RNA-seq, merged into a single network in (A) leaves and (B) roots. Transcription factors are indicated as orange nodes. Complete networks are provided in additional file 1. **Fig. S5** Two potential models for an increased reduction in transcript abundance in the absence of the H_2O_2 -induced Ca^{2+} transient. This could either occur by a regulation of Ca^{2+} -dependent and -independent pathways, which act in opposite directions with different strength of regulation (left panel). Alternatively, the H_2O_2 -induced Ca^{2+} signals might attenuate the H_2O_2 response, so that it becomes stronger in its absence. The arrowheads indicate activation (green) or repression (red)

Supplementary Material 3: **Additional File 3: Table S1** List of primer sequences used for RT-qPCR analyses in this study. Wherever applicable, the corresponding Arabidopsis orthologs are indicated in brackets

Supplementary Material 4: **Additional File 4: Table S2:** Differentially expressed genes (DEGs) between either $\text{H}_2\text{O}_2 + \text{LaCl}_3$ or LaCl_3 and control samples. Differential expression analysis was carried out with the genes using DESeq2. Attached here are the output files obtained after comparing $\text{LaCl}_3 + \text{H}_2\text{O}_2$ treated samples with control samples, in the leaf and the root, along with the DESeq2 output files obtained after comparing LaCl_3 treated samples. DEGs were identified based on adjusted FDR < 0.01 and are listed separately for leaves and roots. Further genes with FDR > 0.01, were considered as genes with unchanged expression (UCs) compared to control samples. Furthermore, the genes commonly regulated between $\text{H}_2\text{O}_2 + \text{LaCl}_3$ and LaCl_3 treatments were excluded to obtain the genes which are unique for $\text{H}_2\text{O}_2 + \text{LaCl}_3$ treatment and presented separately for leaves and roots of barley

Supplementary Material 5: **Additional File 5: Table S3** A comparison of the obtained unique genes in Leaf $\text{H}_2\text{O}_2 + \text{LaCl}_3$ (Table S2) to leaf H_2O_2 -DEGs obtained in our former study (Bhattacharyya et al 2023). For the shared genes between both treatments a selection based on a $\log_2\text{FC}$ difference ($\Delta \log_2\text{FC}$) was performed and only genes showing a $\Delta > 1$ was considered for further analyses. A clustering of the obtained genes resulted in a total of five clusters. control: dd H_2O ; UCs: genes with

unchanged expression vs control

Supplementary Material 6: **Additional File 6: Table S4** A comparison of the obtained unique genes in root H₂O₂+LaCl₃ (Table S2) to root H₂O₂-DEGs obtained in our former study (Bhattacharyya et al 2023). For the shared genes between both treatments a selection based on a log₂FC difference (delta log₂FC) was performed and only genes showing a delta >1 was considered for further analyses. A clustering of the obtained genes resulted in a total of five clusters. control: ddH₂O; UCs: genes with unchanged expression vs control

Acknowledgements

We would like to thank the NGS Core Facility of the Medical Faculty at the University of Bonn for providing support with RNA sequencing platform. Open access publishing ensured by Projekt DEAL. We would also thank Prof. Dr. Kristina Gruden (NIB, Ljubljana, Slovenia) for helpful discussions of the manuscript.

Author contributions

SB contributed to conceptualization, investigation (responsible for most experimental work), formal analysis (responsible for bioinformatic analysis), validation, visualization, and writing - original draft as well as review & editing. EUR and AMB contributed to investigation (RT-qPCR). CB contributed to investigation (network analysis). BM contributed to investigation (Ca²⁺ measurements) and writing - review & editing. MG contributed to investigation. EP contributed to supervision and writing - review and editing. UCV contributed to conceptualization, validation, visualization, funding acquisition, project administration, supervision, and writing - review & editing. FC contributed to conceptualization, formal analysis, validation, visualization, supervision, and writing - original draft as well as review & editing. All authors contributed to the article and approved the submitted version.

Funding

Open Access funding enabled and organized by Projekt DEAL. This work was supported by the Deutsche Forschungsgemeinschaft (INST 217/939-1 FUGG to UCV and GRK 2064 to M.G. and U.V.) and the Slovenian Research Agency (ARIS) under grant agreement Z4-50146 (to CB).

Data availability

Raw RNA-sequencing data used in this study are available in the SRA (Sequence Read Archive) repository from NCBI (<https://www.ncbi.nlm.nih.gov/sra/PRJNA1061386> and <https://www.ncbi.nlm.nih.gov/sra/PRJNA973626>). Code for the network analyses is available on GitHub (<https://github.com/NIB-SI/skm-h2o2-ca2-barley>).

Declarations

Ethical approval and consent to participate

Not applicable.

Consent for publication

Not applicable.

Competing interests

The authors declare no competing interests.

Author details

¹Institute for Cellular and Molecular Botany (IZMB), University of Bonn, Kirschallee 1, D-53115 Bonn, Germany

²Department of Biotechnology and Systems Biology, National Institute of Biology (NIB), Večna pot 111, Ljubljana SI-1000, Slovenia

³Institute of Agricultural and Nutritional Sciences, Faculty of Natural Sciences III, Martin Luther University Halle-Wittenberg, Betty-Heimann-Str. 3, D-06120 Halle (Saale), Germany

⁴Leibniz Institute for Food Systems Biology, Technical University of Munich, Lise-Meitner-Strasse 34, D-85354 Freising, Germany

Received: 1 October 2024 / Accepted: 12 February 2025

Published online: 20 February 2025

References

- Farooq MA, Niazi AK, Akhtar J, Saifullah, Farooq M, Souri Z, et al. Acquiring control: the evolution of ROS-Induced oxidative stress and redox signaling pathways in plant stress responses. *Plant Physiol Biochem.* 2019;141:353–69.
- Huang H, Ullah F, Zhou D-X, Yi M, Zhao Y. Mechanisms of ROS Regulation of Plant Development and stress responses. *Front Plant Sci.* 2019;10.
- Smirnov N, Arnaud D. Hydrogen peroxide metabolism and functions in plants. *New Phytol.* 2019;221:1197–214.
- Choudhury FK, Rivero RM, Blumwald E, Mittler R. Reactive oxygen species, abiotic stress and stress combination. *Plant J.* 2017;90:856–67.
- Waszczak C, Carmody M, Kangasjärvi J. Reactive oxygen species in Plant Signaling. *Annu Rev Plant Biol.* 2018;69:209–36.
- Mittler R, Zandalinas SI, Fichman Y, Van Breusegem F. Reactive oxygen species signalling in plant stress responses. *Nat Rev Mol Cell Biol.* 2022;23:663–79.
- Mittler R. ROS are good. *Trends Plant Sci.* 2017;22:11–9.
- Mhamdi A, Van Breusegem F. Reactive oxygen species in plant development. *Development.* 2018;145:dev164376.
- Dumanović J, Nepovimova E, Natić M, Kuča K, Jačević V. The significance of reactive oxygen species and antioxidant defense system in plants: a concise overview. *Front Plant Sci.* 2021;11.
- Liao W, Xiao H, Zhang M. Role and relationship of nitric oxide and hydrogen peroxide in adventitious root development of marigold. *Acta Physiol Plant.* 2009;31:1279–89.
- Hernández-Barrera A, Velarde-Buendía A, Zepeda I, Sanchez F, Quinto C, Sánchez-Lopez R, et al. Hyper, a Hydrogen Peroxide Sensor, indicates the sensitivity of the Arabidopsis Root Elongation Zone to Aluminum Treatment. *Sensors.* 2015;15:855–67.
- Liu J, Macarasin D, Wisniewski M, Sui Y, Droby S, Norelli J, et al. Production of hydrogen peroxide and expression of ROS-generating genes in peach flower petals in response to host and non-host fungal pathogens. *Plant Pathol.* 2013;62:820–8.
- Barba-Espin G, Diaz-Vivancos P, Job D, Belghazi M, Job C, Hernández JA. Understanding the role of H₂O₂ during pea seed germination: a combined proteomic and hormone profiling approach. *Plant Cell Environ.* 2011;34:1907–19.
- Liao W-B, Zhang M-L, Huang G-B, Yu J-H. Hydrogen peroxide in the vase solution increases vase life and keeping quality of cut Oriental Trumpet hybrid lily 'Manissa'. *Sci Hort.* 2012;139:32–8.
- Ge X-M, Cai H-L, Lei X, Zhou X, Yue M, He J-M. Heterotrimeric G protein mediates ethylene-induced stomatal closure via hydrogen peroxide synthesis in Arabidopsis. *Plant J.* 2015;82:138–50.
- Hameed A, Iqbal N. Chemo-priming with mannose, mannitol and H₂O₂ mitigate drought stress in wheat. *Cereal Res Commun.* 2014;42:450–62.
- Ashraf MA, Rasheed R, Hussain I, Iqbal M, Haider MZ, Parveen S, et al. Hydrogen peroxide modulates antioxidant system and nutrient relation in maize (*Zea mays* L.) under water-deficit conditions. *Arch Agron Soil Sci.* 2015;61:507–23.
- Sathiyaraj G, Srinivasan S, Kim Y-J, Lee OR, Parvin S, Balusamy SRD, et al. Acclimation of hydrogen peroxide enhances salt tolerance by activating defense-related proteins in Panax ginseng C.A. Meyer. *Mol Biol Rep.* 2014;41:3761–71.
- Wang Y, Zhang J, Li J-L, Ma X-R. Exogenous hydrogen peroxide enhanced the thermotolerance of *Festuca arundinacea* and *Lolium perenne* by increasing the antioxidative capacity. *Acta Physiol Plant.* 2014;36:2915–24.
- Wu D, Chu H, Jia L, Chen K, Zhao L. A feedback inhibition between nitric oxide and hydrogen peroxide in the heat shock pathway in Arabidopsis seedlings. *Plant Growth Regul.* 2015;75:503–9.
- Czégény G, Wu M, Dér A, Eriksson LA, Strid Å, Hideg É. Hydrogen peroxide contributes to the ultraviolet-B (280–315nm) induced oxidative stress of plant leaves through multiple pathways. *FEBS Lett.* 2014;588:2255–61.
- Oksanen E, Häikiö E, Sober J, Karnosky DF. Ozone-induced H₂O₂ accumulation in field-grown aspen and birch is linked to foliar ultrastructure and peroxisomal activity. *New Phytol.* 2004;161:791–9.
- Xu A, Cheng F, Zhou S, Hu H, Bie Z. Chilling-induced H₂O₂ signaling activates the antioxidant enzymes in alleviating the photooxidative damage caused by loss of function of 2-Cys peroxiredoxin in watermelon. *Plant Stress.* 2022;6:100108.
- Wen J-F, Gong M, Liu Y, Hu J-L, Deng M. Effect of hydrogen peroxide on growth and activity of some enzymes involved in proline metabolism of sweet corn seedlings under copper stress. *Sci Hort.* 2013;164:366–71.
- Shetty NP, Jørgensen HJL, Jensen JD, Collinge DB, Shetty HS. Roles of reactive oxygen species in interactions between plants and pathogens. *Eur J Plant Pathol.* 2008;121:267–80.

26. Nadarajah KK. Defensive strategies of ROS in Plant–Pathogen interactions. In: Verma PK, Mishra S, Srivastava V, Mehrotra S, editors. *Plant Pathogen Interaction*. Singapore: Springer Nature Singapore; 2023. pp. 163–83.
27. Hu C-H, Wang P-Q, Zhang P-P, Nie X-M, Li B-B, Tai L et al. NADPH oxidases: the vital performers and Center hubs during Plant Growth and Signaling. *Cells*. 2020;9.
28. Manishankar P, Wang N, Köster P, Alatar AA, Kudla J. Calcium signaling during salt stress and in the regulation of ion homeostasis. *J Exp Bot*. 2018;69:4215–26.
29. Seifikalhor M, Aliniaiefard S, Shomali A, Azad N, Hassani B, Lastochkina O, et al. Calcium signaling and salt tolerance are diversely entwined in plants. *Plant Signal Behav*. 2019;14:1665455.
30. Yuan P, Yang T, Poovaiah BW. Calcium signaling-mediated plant response to cold stress. *Int J Mol Sci*. 2018;19.
31. Iqbal Z, Memon AG, Ahmad A, Iqbal MS. Calcium mediated cold acclimation in plants: Underlying Signaling and Molecular mechanisms. *Front Plant Sci*. 2022;13.
32. Knight H, Trewavas AJ, Knight MR. Calcium signalling in *Arabidopsis thaliana* responding to drought and salinity. *Plant J*. 1997;12:1067–78.
33. Knight H, Brandt S, Knight MR. A history of stress alters drought calcium signalling pathways in. *Plant J*. 1998;16:681–7.
34. Shao H-B, Song W-Y, Chu L-Y. Advances of calcium signals involved in plant anti-drought. *CR Biol*. 2008;331:587–96.
35. Guihur A, Rebeaud ME, Goloubinoff P. How do plants feel the heat and survive? *Trends Biochem Sci*. 2022;47:824–38.
36. Kang X, Zhao L, Liu X. Calcium Signaling and the response to heat shock in crop plants. *Int J Mol Sci*. 2024;25.
37. Jalmi SK, Bhagat PK, Verma D, Noryang S, Tayyeba S, Singh K et al. Traversing the links between Heavy Metal Stress and Plant Signaling. *Front Plant Sci*. 2018;9.
38. Aldon D, Mbengue M, Mazars C, Galaud J-P. Calcium signalling in plant biotic interactions. *Int J Mol Sci*. 2018;19.
39. Negi NP, Prakash G, Narwal P, Panwar R, Kumar D, Chaudhry B et al. The calcium connection: exploring the intricacies of calcium signaling in plant-microbe interactions. *Front Plant Sci*. 2023;14.
40. Ranty B, Aldon D, Cotellet V, Galaud J-P, Thuleau P, Mazars C. Calcium sensors as key hubs in plant responses to biotic and abiotic stresses. *Front Plant Sci*. 2016;7.
41. Ren H, Zhang Y, Zhong M, Hussian J, Tang Y, Liu S, et al. Calcium signaling-mediated transcriptional reprogramming during abiotic stress response in plants. *Theor Appl Genet*. 2023;136:210.
42. Marcec MJ, Gilroy S, Poovaiah BW, Tanaka K. Mutual interplay of Ca²⁺ and ROS signaling in plant immune response. *Plant Sci*. 2019;283:343–54.
43. Ravi B, Foyer CH, Pandey GK. The integration of reactive oxygen species (ROS) and calcium signalling in abiotic stress responses. *Plant Cell Environ*. 2023;46:1985–2006.
44. Kobayashi M, Ohura I, Kawakita K, Yokota N, Fujiwara M, Shimamoto K, et al. Calcium-dependent protein kinases regulate the production of reactive oxygen species by potato NADPH oxidase. *Plant Cell*. 2007;19:1065–80.
45. Ogasawara Y, Kaya H, Hiraoka G, Yumoto F, Kimura S, Kadota Y, et al. Synergistic activation of the Arabidopsis NADPH oxidase AtrbohD by Ca²⁺ and phosphorylation. *J Biol Chem*. 2008;283:8885–92.
46. Dubiella U, Seybold H, Durian G, Komander E, Lassig R, Witte C-P, et al. Calcium-dependent protein kinase/NADPH oxidase activation circuit is required for rapid defense signal propagation. *Proc Natl Acad Sci*. 2013;110:8744–9.
47. Pei Z-M, Murata Y, Benning G, Thomine S, Klüsener B, Allen GJ, et al. Calcium channels activated by hydrogen peroxide mediate abscisic acid signalling in guard cells. *Nature*. 2000;406:731–4.
48. Rentel MC, Knight MR. Oxidative stress-Induced Calcium Signaling in Arabidopsis. *Plant Physiol*. 2004;135:1471–9.
49. Lecourieux D, Ranjeva R, Pugin A. Calcium in plant defence-signalling pathways. *New Phytol*. 2006;171:249–69.
50. Demidchik V, Shabala S, Isayenkov S, Cuin TA, Pottosin I. Calcium transport across plant membranes: mechanisms and functions. *New Phytol*. 2018;220:49–69.
51. Fichman Y, Zandalinas SI, Peck S, Luan S, Mittler R. HPCA1 is required for systemic reactive oxygen species and calcium cell-to-cell signaling and plant acclimation to stress. *Plant Cell*. 2022;34:4453–71.
52. Wu F, Chi Y, Jiang Z, Xu Y, Xie L, Huang F, et al. Hydrogen peroxide sensor HPCA1 is an LRR receptor kinase in Arabidopsis. *Nature*. 2020;578:577–81.
53. Gürel F, Öztürk ZN, Uçarlı C, Rosellini D. Barley genes as tools to Confer Abiotic stress tolerance in crops. *Front Plant Sci*. 2016;7.
54. Holubová K, Hensel G, Vojta P, Tarkowski P, Bergougnoux V, Galuszka P. Modification of Barley Plant Productivity through Regulation of Cytokinin Content by Reverse-Genetics approaches. *Front Plant Sci*. 2018;9.
55. Bhattacharyya S, Giridhar M, Meier B, Peiter E, Vothknecht UC, Chigri F. Global transcriptome profiling reveals root- and leaf-specific responses of barley (*Hordeum vulgare* L.) to H₂O₂. *Front Plant Sci*. 2023;14.
56. Giridhar M, Meier B, Imani J, Kogel K-H, Peiter E, Vothknecht UC, et al. Comparative analysis of stress-induced calcium signals in the crop species barley and the model plant Arabidopsis thaliana. *BMC Plant Biol*. 2022;22:447.
57. Kaur N, Dhawan M, Sharma I, Pati PK. Interdependency of reactive oxygen species generating and scavenging system in salt sensitive and salt tolerant cultivars of rice. *BMC Plant Biol*. 2016;16:131.
58. Moll P, Ante M, Seitz A, Reda T. QuantSeq 3' mRNA sequencing for RNA quantification. *Nat Methods*. 2014;11:i–iii.
59. Team RC. Version 4.3.2., 2023. <https://www.r-project.org/>
60. Love MI, Huber W, Anders S. Moderated estimation of Fold change and dispersion for RNA-seq data with DESeq2. *Genome Biol*. 2014;15:550.
61. Mascher M, Gundlach H, Himmelfach A, Beier S, Twardziok SO, Wicker T, et al. A chromosome conformation capture ordered sequence of the barley genome. *Nature*. 2017;544:427–33.
62. Li Y, Wu H. A clustering method based on K-Means Algorithm. *Physics Procedia*. 2012;25:1104–9.
63. Handhayani T, Hiryanto L. Intelligent Kernel K-Means for Clustering Gene expression. *Procedia Comput Sci*. 2015;59:171–7.
64. Tibshirani R, Walther G, Hastie T. Estimating the number of clusters in a data set via the gap statistic. *J Royal Stat Society: Ser B (Statistical Methodology)*. 2001;63:411–23.
65. Bleker C, Ramšak Ž, Bittner A, Podpečan V, Zagoščak M, Wurzing B, et al. Stress knowledge map: a knowledge graph resource for systems biology analysis of plant stress responses. *Plant Commun*. 2024;5:100920.
66. Ramšak Ž, Baebler Š, Rotter A, Korbar M, Mozetič I, Usadel B, et al. GoMapMan: integration, consolidation and visualization of plant gene annotations within the MapMan ontology. *Nucleic Acids Res*. 2014;42:D1167–75.
67. Hagberg AA, Schult DA, Swart PJ. Exploring network structure, dynamics, and function using NetworkX. In: *Proceedings of the 7th Python in Science Conference (SciPy2008)*. Pasadena, California. pp. 11–5.
68. Peixoto TP. The graph-tool python library. 2014.
69. Cline MS, Smoot M, Cerami E, Kuchinsky A, Landys N, Workman C, et al. Integration of biological networks and gene expression data using Cytoscape. *Nat Protoc*. 2007;2:2366–82.
70. Gustavsen J, Pai S, Isserlin R, Demchak B, Pico A. RCy3: Network biology using Cytoscape from within R [version 3; peer review: 3 approved]. *F1000Research*. 2019;8.
71. Livak KJ, Schmittgen TD. Analysis of relative gene expression data using real-time quantitative PCR and the 2^{-ΔΔCT} method. *Methods*. 2001;25:402–8.
72. Bui LT, Giuntoli B, Kosmacz M, Parlanti S, Licausi F. Constitutively expressed ERF-VII transcription factors redundantly activate the core anaerobic response in Arabidopsis thaliana. *Plant Sci*. 2015;236:37–43.
73. Gibbs DJ, Conde JV, Berckhan S, Prasad G, Mendiondo GM, Holdsworth MJ. Group VII Ethylene Response Factors Coordinate Oxygen and Nitric Oxide Signal Transduction and stress responses in plants. *Plant Physiol*. 2015;169:23–31.
74. Xie Z, Nolan TM, Jiang H, Yin Y. AP2/ERF Transcription Factor Regulatory Networks in hormone and abiotic stress responses in Arabidopsis. *Front Plant Sci*. 2019;10.
75. Rushton DL, Tripathi P, Rabara RC, Lin J, Ringler P, Boken AK, et al. WRKY transcription factors: key components in abscisic acid signalling. *Plant Biotechnol J*. 2012;10:2–11.
76. Nuruzzaman M, Sharoni AM, Kikuchi S. Roles of NAC transcription factors in the regulation of biotic and abiotic stress responses in plants. *Front Microbiol*. 2013;4.
77. Khoso MA, Hussain A, Ritonga FN, Ali Q, Channa MM, Alshegaih RM et al. WRKY transcription factors (TFs): molecular switches to regulate drought, temperature, and salinity stresses in plants. *Front Plant Sci*. 2022;13.
78. Koo AJK, Cooke TF, Howe GA. Cytochrome P450 CYP94B3 mediates catabolism and inactivation of the plant hormone jasmonoyl-L-isoleucine. *Proceedings of the National Academy of Sciences*. 2011;108:9298–303.
79. Heitz T, Widemann E, Lugan R, Miesch L, Ullmann P, Désaubry L, et al. Cytochromes P450 CYP94C1 and CYP94B3 catalyze two successive oxidation steps of plant hormone jasmonoyl-isoleucine for catabolic turnover. *J Biol Chem*. 2012;287:6296–306.

80. Lorenzo O, Piqueras R, Sánchez-Serrano JJ, Solano R. ETHYLENE RESPONSE FACTOR1 integrates signals from Ethylene and Jasmonate pathways in Plant Defense. *Plant Cell*. 2003;15:165–78.
81. Kagaya Y, Hattori T. Arabidopsis transcription factors, RAV1 and RAV2, are regulated by touch-related stimuli in a dose-dependent and biphasic manner. *Genes Genet Syst*. 2009;84:95–9.
82. Bourdais G, Burdiak P, Gauthier A, Nitsch L, Salojärvi J, Rayapuram C, et al. Large-scale Phenomics identifies primary and fine-tuning roles for CRKs in responses related to oxidative stress. *PLoS Genet*. 2015;11:e1005373.
83. Hoffmann N. Setting the stage for lignin deposition: spatial distribution of enzymes directing lignification in *Arabidopsis thaliana*. Text. 2019.
84. Wang F, Yu G, Liu P. Transporter-mediated subcellular distribution in the metabolism and signaling of Jasmonates. *Front Plant Sci*. 2019;10.
85. Tessi TM, Brumm S, Winklbauer E, Schumacher B, Pettinari G, Lescano I, et al. Arabidopsis AZG2 transports cytokinins in vivo and regulates lateral root emergence. *New Phytol*. 2021;229:979–93.
86. Hartmann M, Zeier T, Bernsdorff F, Reichel-Deland V, Kim D, Hohmann M, et al. Flavin Monooxygenase-generated N-Hydroxypipicolinic acid is a critical element of plant systemic immunity. *Cell*. 2018;173:456–e46916.
87. Czarnocka W, Fichman Y, Bernacki M, Róžańska E, Sańko-Sawczenko I, Mittler R et al. FMO1 is involved in excess light stress-Induced Signal Transduction and Cell Death Signaling. *Cells*. 2020;9.
88. Guerra T, Schilling S, Hake K, Gorzalka K, Sylvestre F-P, Conrads B, et al. Calcium-dependent protein kinase 5 links calcium signaling with N-hydroxy-L-pipicolinic acid- and SARD1-dependent immune memory in systemic acquired resistance. *New Phytol*. 2020;225:310–25.
89. Gasch P, Fundinger M, Müller JT, Lee T, Bailey-Serres J, Mustroph A. Redundant ERF-VII transcription factors bind to an evolutionarily conserved cis-motif to regulate hypoxia-responsive gene expression in Arabidopsis. *Plant Cell*. 2016;28:160–80.
90. Klecker M, Gasch P, Peisker H, Dörmann P, Schlicke H, Grimm B, et al. A shoot-specific hypoxic response of Arabidopsis sheds light on the role of the phosphate-responsive transcription factor PHOSPHATE STARVATION RESPONSE1. *Plant Physiol*. 2014;165:774–90.
91. Valliyodan B, Van Toai TT, Alves JD, De Fátima P, Goulart P, Lee JD, Fritschi FB, et al. Expression of Root-Related Transcription Factors Associated with flooding tolerance of soybean (*Glycine max*). *Int J Mol Sci*. 2014;15:17622–43.
92. Bittner A, Cieřla A, Gruden K, Lukan T, Mahmud S, Teige M, et al. Organelles and phytohormones: a network of interactions in plant stress responses. *J Exp Bot*. 2022;73:7165–81.
93. Yang T-H, Lenglet-Hilffker A, Stolz S, Glauser G, Farmer EE. Jasmonate Precursor Biosynthetic enzymes LOX3 and LOX4 control wound-response growth restriction. *Plant Physiol*. 2020;184:1172–80.
94. Ozalvo R, Cabrera J, Escobar C, Christensen SA, Borrego EJ, Kolomiets MV, et al. Two closely related members of Arabidopsis 13-lipoxygenases (13-LOXs), LOX3 and LOX4, reveal distinct functions in response to plant-parasitic nematode infection. *Mol Plant Pathol*. 2014;15:319–32.
95. Ding H, Lai J, Wu Q, Zhang S, Chen L, Dai Y-S, et al. Jasmonate complements the function of Arabidopsis lipoxygenase3 in salinity stress response. *Plant Sci*. 2016;244:1–7.
96. Rieu I, Ruiz-Rivero O, Fernandez-García N, Griffiths J, Powers SJ, Gong F, et al. The gibberellin biosynthetic genes AtGA20ox1 and AtGA20ox2 act, partially redundantly, to promote growth and development throughout the Arabidopsis life cycle. *Plant J*. 2008;53:488–504.
97. Jaradat MR, Feurtado JA, Huang D, Lu Y, Cutler AJ. Multiple roles of the transcription factor AtMYB1/ATMYB44 in ABA signaling, stress responses, and leaf senescence. *BMC Plant Biol*. 2013;13:192.
98. Shim JS, Jung C, Lee S, Min K, Lee Y-W, Choi Y, et al. AtMYB44 regulates WRKY70 expression and modulates antagonistic interaction between salicylic acid and jasmonic acid signaling. *Plant J*. 2013;73:483–95.
99. Llorente F, López-Cobollo RM, Catalá R, Martínez-Zapater JM, Salinas J. A novel cold-inducible gene from Arabidopsis, RCI3, encodes a peroxidase that constitutes a component for stress tolerance. *Plant J*. 2002;32:13–24.
100. Kim BH, Kim SY, Nam KH. Genes encoding plant-specific class III peroxidases are responsible for increased cold tolerance of the brassinosteroid-insensitive 1 mutant. *Mol Cells*. 2012;34:539–48.
101. Al-Quraan NA, Locy RD, Singh NK. Expression of calmodulin genes in wild type and calmodulin mutants of Arabidopsis thaliana under heat stress. *Plant Physiol Biochem*. 2010;48:697–702.
102. Evans MJ, Choi W-G, Gilroy S, Morris RJ. A ROS-Assisted calcium Wave Dependent on the ATRBOHD NADPH oxidase and TPC1 Cation Channel propagates the systemic response to salt stress. *Plant Physiol*. 2016;171:1771–84.
103. Liu N, Hake K, Wang W, Zhao T, Romeis T, Tang D. CALCIUM-DEPENDENT PROTEIN KINASE5 associates with the truncated NLR protein TIR-NBS2 to contribute to exo70B1-Mediated immunity. *Plant Cell*. 2017;29:746–59.
104. Jammes F, Song C, Shin D, Munemasa S, Takeda K, Gu D, et al. MAP kinases MPK9 and MPK12 are preferentially expressed in guard cells and positively regulate ROS-mediated ABA signaling. *Proc Natl Acad Sci*. 2009;106:20520–5.
105. Desikan R, Horák J, Chaban C, Mira-Rodado V, Witthöft J, Elgass K, et al. The histidine kinase AHK5 integrates endogenous and Environmental Signals in Arabidopsis Guard cells. *PLoS ONE*. 2008;3:e2491.
106. Rao S, Zhou Z, Miao P, Bi G, Hu M, Wu Y, et al. Roles of receptor-like cytoplasmic kinase VII members in pattern-triggered Immune Signaling. *Plant Physiol*. 2018;177:1679–90.
107. Song C, Lee J, Kim T, Hong JC, Lim CO. VOZ1, a transcriptional repressor of DREB2C, mediates heat stress responses in Arabidopsis. *Planta*. 2018;247:1439–48.
108. Sylvestre-Gonon E, Law SR, Schwartz M, Robe K, Keech O, Didierjean C et al. Functional, structural and biochemical features of plant serinyl-glutathione transferases. *Front Plant Sci*. 2019;10.
109. Solano R, Stepanova A, Chao Q, Ecker JR. Nuclear events in ethylene signaling: a transcriptional cascade mediated by ETHYLENE-INSENSITIVE3 and ETHYLENE-RESPONSE-FACTOR1. *Genes Dev*. 1998;12:3703–14.
110. Houben B, Vaughan-Hirsch J, Pattyn J, Mou W, Roden S, Martinez Roig A, et al. 1-Aminocyclopropane-1-carboxylic acid oxidase determines the fate of ethylene biosynthesis in a tissue-specific way to fine-tune development and stress resilience. *bioRxiv*. 2024. 2024.02.01.578397.
111. Romero-Hernandez G, Martinez M. Plant Kinases in the Perception and Signaling Networks Associated with Arthropod Herbivory. *Front Plant Sci*. 2022;13.
112. Chu M, Chen P, Meng S, Xu P, Lan W. The Arabidopsis phosphatase PP2C49 negatively regulates salt tolerance through inhibition of AtHKT1;1. *J Integr Plant Biol*. 2021;63:528–42.
113. Moyet L, Salvi D, Bouchnak I, Miras S, Perrot L, Seigneurin-Berny D, et al. Calmodulin is involved in the dual subcellular location of two chloroplast proteins. *J Biol Chem*. 2019;294:17543–54.
114. Fasani E, DalCorso G, Costa A, Zenoni S, Furini A. The Arabidopsis thaliana transcription factor MYB59 regulates calcium signalling during plant growth and stress response. *Plant Mol Biol*. 2019;99:517–34.
115. Lee S, Wang W, Huq E. Spatial regulation of thermomorphogenesis by HY5 and PIF4 in Arabidopsis. *Nat Commun*. 2021;12:3656.
116. Agarwal P, Mitra M, Banerjee S, Roy S. MYB4 transcription factor, a member of R2R3-subfamily of MYB domain protein, regulates cadmium tolerance via enhanced protection against oxidative damage and increases expression of PCS1 and MT1C in Arabidopsis. *Plant Sci*. 2020;297:110501.
117. Wang X-C, Wu J, Guan M-L, Zhao C-H, Geng P, Zhao Q. Arabidopsis MYB4 plays dual roles in flavonoid biosynthesis. *Plant J*. 2020;101:637–52.
118. Yuan F, Yang H, Xue Y, Kong D, Ye R, Li C, et al. OSCA1 mediates osmotic-stress-evoked Ca²⁺ increases vital for osmosensing in Arabidopsis. *Nature*. 2014;514:367–71.
119. Asaoka R, Uemura T, Ito J, Fujimoto M, Ito E, Ueda T, et al. Arabidopsis RABA1 GTPases are involved in transport between the trans-golgi network and the plasma membrane, and are required for salinity stress tolerance. *Plant J*. 2013;73:240–9.
120. Tak H, Negi S, Ganapathi TR. Banana NAC transcription factor MusaNAC042 is positively associated with drought and salinity tolerance. *Protoplasma*. 2017;254:803–16.
121. Alshareef NO, Wang JY, Ali S, Al-Babili S, Tester M, Schmöckel SM. Overexpression of the NAC transcription factor JUNGBRUNNEN1 (JUB1) increases salinity tolerance in tomato. *Plant Physiol Biochem*. 2019;140:113–21.
122. Noman M, Aysha J, Keteouli T, Yang J, Du L, Wang F, et al. Calmodulin binding transcription activators: an interplay between calcium signalling and plant stress tolerance. *J Plant Physiol*. 2021;256:153327.
123. Perochon A, Aldon D, Galaud J-P, Ranty B. Calmodulin and calmodulin-like proteins in plant calcium signaling. *Biochimie*. 2011;93:2048–53.
124. Dekomah SD, Bi Z, Dormatey R, Wang Y, Haider FU, Sun C et al. The role of CDPKs in plant development, nutrient and stress signaling. *Front Genet*. 2022;13.
125. Liu L, White MJ, MacRae TH. Transcription factors and their genes in higher plants. *Eur J Biochem*. 1999;262:247–57.
126. Evans KV, Ransom E, Nayakoti S, Wilding B, Mohd Salleh F, Gržina I, et al. Expression of the Arabidopsis redox-related LEA protein, SAG21 is regulated by ERF, NAC and WRKY transcription factors. *Sci Rep*. 2024;14:7756.

127. Verma V, Ravindran P, Kumar PP. Plant hormone-mediated regulation of stress responses. *BMC Plant Biol.* 2016;16:86.
128. Xu W, Huang W. Calcium-dependent protein kinases in Phytohormone Signaling pathways. *Int J Mol Sci.* 2017;18.
129. Zhu Q, Feng Y, Xue J, Chen P, Zhang A, Yu Y. Advances in receptor-like protein kinases in balancing plant growth and stress responses. *Plants.* 2023;12.
130. Le Gall H, Philippe F, Domon J-M, Gillet F, Pelloux J, Rayon C. Cell wall metabolism in response to Abiotic Stress. *Plants.* 2015;4:112–66.
131. Tenhaken R. Cell wall remodeling under abiotic stress. *Front Plant Sci.* 2015;5.
132. Liu W-C, Han T-T, Yuan H-M, Yu Z-D, Zhang L-Y, Zhang B-L, et al. Functions for seedling postgerminative growth by scavenging HO and stimulating ACX2/3 activity in. *Plant Cell Environ.* 2017;40:2720–8.
133. Kapilan R, Vaziri M, Zwiazek JJ. Regulation of aquaporins in plants under stress. *Biol Res.* 2018;51:4.
134. Chopra D, Hasan MS, Matera C, Chitambo O, Mendy B, Mahlitz S-V, et al. Plant parasitic cyst nematodes redirect host indole metabolism via NADPH oxidase-mediated ROS to promote infection. *New Phytol.* 2021;232:318–31.
135. Lohse S, Schliemann W, Ammer C, Kopka J, Strack D, Fester T. Organization and Metabolism of Plastids and Mitochondria in Arbuscular Mycorrhizal roots of *Medicago truncatula*. *Plant Physiol.* 2005;139:329–40.
136. Janiak A, Kwasniewski M, Sowa M, Gajek K, Żmuda K, Kościelniak J et al. No time to Waste: Transcriptome Study reveals that Drought Tolerance in Barley May be attributed to stressed-like expression patterns that exist before the occurrence of stress. *Front Plant Sci.* 2018;8.
137. Kobayashi K, Sasaki D, Noguchi K, Fujinuma D, Komatsu H, Kobayashi M, et al. Photosynthesis of Root chloroplasts developed in Arabidopsis Lines Overexpressing GOLDEN2-LIKE transcription factors. *Plant Cell Physiol.* 2013;54:1365–77.
138. Dolgikh VA, Pukhovaya EM, Zemlyanskaya EV. Shaping Ethylene response: the role of EIN3/EIL1 transcription factors. *Front Plant Sci.* 2019;10.
139. Lang T, Deng C, Yao J, Zhang H, Wang Y, Deng S. A Salt-Signaling Network Involving Ethylene, Extracellular ATP, Hydrogen Peroxide, and Calcium mediates K^+/Na^+ homeostasis in Arabidopsis. *Int J Mol Sci.* 2020;21.
140. Kumari P, Dahiya P, Livanos P, Zergiebel L, Kölling M, Poeschl Y, et al. IQ67 DOMAIN proteins facilitate preprophase band formation and division-plane orientation. *Nat Plants.* 2021;7:739–47.
141. Xiao Y, Chu L, Zhang Y, Bian Y, Xiao J, Xu D. HYS: A Pivotal Regulator of Light-Dependent Development in higher plants. *Front Plant Sci.* 2022;12.
142. Bellegarde F, Maghiaoui A, Boucherez J, Krouk G, Lejay L, Bach L et al. HNI9 and HYS maintain ROS homeostasis under high nitrogen provision in Arabidopsis. *bioRxiv.* 2018;479030.
143. Li J, Zeng J, Tian Z, Zhao Z. Root-specific photoreception directs early root development by HY5-regulated ROS balance. *Proceedings of the National Academy of Sciences.* 2024;121:e2313092121.
144. Abbas N, Maurya JP, Senapati D, Gangappa SN, Chattopadhyay S. Arabidopsis CAM7 and HY5 physically interact and directly bind to the HY5 promoter to regulate its expression and thereby promote photomorphogenesis. *Plant Cell.* 2014;26:1036–52.
145. Giri MK, Singh N, Banday ZZ, Singh V, Ram H, Singh D, et al. GBF1 differentially regulates 2 and 4 transcription to promote pathogen defense in Arabidopsis thaliana. *Plant J.* 2017;91:802–15.
146. Dóczy R, Brader G, Pettkó-Szandtner A, Rajh I, Djamei A, Pitzschke A, et al. The Arabidopsis Mitogen-activated protein kinase kinase MKK3 is Upstream of Group C Mitogen-Activated Protein Kinases and participates in Pathogen Signaling. *Plant Cell.* 2007;19:3266–79.
147. Popescu SC, Popescu GV, Bachan S, Zhang Z, Seay M, Gerstein M et al. Differential binding of calmodulin-related proteins to their targets revealed through high-density Arabidopsis protein microarrays. *Proceedings of the National Academy of Sciences.* 2007;104:4730–5.
148. Liu Z, Guo C, Wu R, Hu Y, Zhou Y, Wang J et al. FLS2-RBOHD-PIF4 Module regulates Plant Response to Drought and Salt stress. *Int J Mol Sci.* 2022;23.
149. Stamm P, Ravindran P, Mohanty B, Tan EL, Yu H, Kumar PP. Insights into the molecular mechanism of RGL2-mediated inhibition of seed germination in *Arabidopsis thaliana*. *BMC Plant Biol.* 2012;12:179.
150. Ali F, Qanmber G, Li F, Wang Z. Updated role of ABA in seed maturation, dormancy, and germination. *J Adv Res.* 2022;35:199–214.
151. Puglia GD. Reactive oxygen and nitrogen species (RONS) signalling in seed dormancy release, perception of environmental cues, and heat stress response. *Plant Growth Regul.* 2024;103:9–32.
152. Denison FC, Paul A-L, Zupanska AK, Ferl RJ. 14-3-3 proteins in plant physiology. *Semin Cell Dev Biol.* 2011;22:720–7.
153. Yang Z, Wang C, Xue Y, Liu X, Chen S, Song C, et al. Calcium-activated 14-3-3 proteins as a molecular switch in salt stress tolerance. *Nat Commun.* 2019;10:1199.

Publisher's note

Springer Nature remains neutral with regard to jurisdictional claims in published maps and institutional affiliations.